Cell

Article

Transkingdom Control of Microbiota Diurnal Oscillations Promotes Metabolic Homeostasis

Christoph A. Thaiss,[1] David Zeevi,[2] Maayan Levy,[1] Gili Zilberman-Schapira,[1] Jotham Suez,[1] Anouk C. Tengeler,[1] Lior Abramson,[1] Meirav N. Katz,[1,3] Tal Korem,[2] Niv Zmora,[3,4,5] Yael Kuperman,[6] Inbal Biton,[6] Shlomit Gilad,[7] Alon Harmelin,[6] Hagit Shapiro,[1] Zamir Halpern,[3,5] Eran Segal,[2] and Eran Elinav[1,*]

[1]Department of Immunology, Weizmann Institute of Science, Rehovot 76100, Israel

[2]Department of Computer Science and Applied Mathematics, Weizmann Institute of Science, Rehovot 76100, Israel

[3]Research Center for Digestive Tract and Liver Diseases, Tel Aviv Sourasky Medical Center, Sackler Faculty of Medicine, Tel Aviv University, Tel Aviv 69978, Israel

[4]Internal Medicine Department, Tel Aviv Sourasky Medical Center, Tel Aviv 64239, Israel

[5]Digestive Center, Tel Aviv Sourasky Medical Center, Tel Aviv 64239, Israel

[6]Department of Veterinary Resources, Weizmann Institute of Science, Rehovot 76100, Israel

[7]The Nancy and Stephen Grand Israel National Center for Personalized Medicine (INCPM), Weizmann Institute of Science, Rehovot 76100, Israel

*Correspondence: eran.elinav@weizmann.ac.il

http://dx.doi.org/10.1016/j.cell.2014.09.048

SUMMARY

All domains of life feature diverse molecular clock machineries that synchronize physiological processes to diurnal environmental fluctuations. However, no mechanisms are known to cross-regulate prokaryotic and eukaryotic circadian rhythms in multikingdom ecosystems. Here, we show that the intestinal microbiota, in both mice and humans, exhibits diurnal oscillations that are influenced by feeding rhythms, leading to time-specific compositional and functional profiles over the course of a day. Ablation of host molecular clock components or induction of jet lag leads to aberrant microbiota diurnal fluctuations and dysbiosis, driven by impaired feeding rhythmicity. Consequently, jet-lag-induced dysbiosis in both mice and humans promotes glucose intolerance and obesity that are transferrable to germ-free mice upon fecal transplantation. Together, these findings provide evidence of coordinated metaorganism diurnal rhythmicity and offer a microbiome-dependent mechanism for common metabolic disturbances in humans with aberrant circadian rhythms, such as those documented in shift workers and frequent flyers.

INTRODUCTION

Life on Earth is dictated by circadian fluctuations of light caused by the planet's rotation around its own axis. Biological clocks are oscillators that enable the anticipation of diurnal variations in environmental conditions and thereby couple physiological processes to geophysical time (Mohawk et al., 2012). All three domains of life —archaea, bacteria, and eukarya—have evolved different methods of developing molecular machineries to coordinate this task (Edgar et al., 2012).

The mammalian circadian clock consists of several core transcriptional regulators, including CLOCK and BMAL1, which are most abundant during the light phase, as well as cryptochromes (CRYs) and period proteins (PERs), which are most highly expressed during the dark phase (Bass, 2012). The circadian clock is characterized by a hierarchical principle. The central clock in the suprachiasmatic nucleus is entrained by environmental light conditions. In turn, the central clock entrains the peripheral clocks through various hormonal and neuronal signals, which dictate the rhythmic gene expression of oscillating genes in most other organ systems (Dibner et al., 2010; Hogenesch and Ueda, 2011). In the periphery, the circadian clock controls many biological processes, ranging from metabolism and behavior to immunity, and helps to synchronize these processes to diurnal fluctuations in environmental conditions (Asher et al., 2010; Gerhart-Hines et al., 2013; Keller et al., 2009; Nguyen et al., 2013; Silver et al., 2012; Yu et al., 2013).

In humans, disruption of the circadian clock is a common hallmark of the modern alteration in lifestyle and is especially evident in individuals engaged in chronic shift work or frequently flying across time zones and experiencing the "jet lag" phenomenon. This new set of disruptive conditions to human physiology is associated with a propensity for a wide range of diseases, including obesity, diabetes, cancer, cardiovascular disease, and susceptibility to infection (Archer et al., 2014; Buxton et al., 2012; Fonken et al., 2010; Scheer et al., 2009; Suwazono et al., 2008). The mechanisms by which disruption of circadian rhythmicity contributes to these pathophysiological outcomes remain largely unknown.

The bacterial circadian clock has primarily been studied in light-responsive cyanobacterial communities (Johnson et al.,

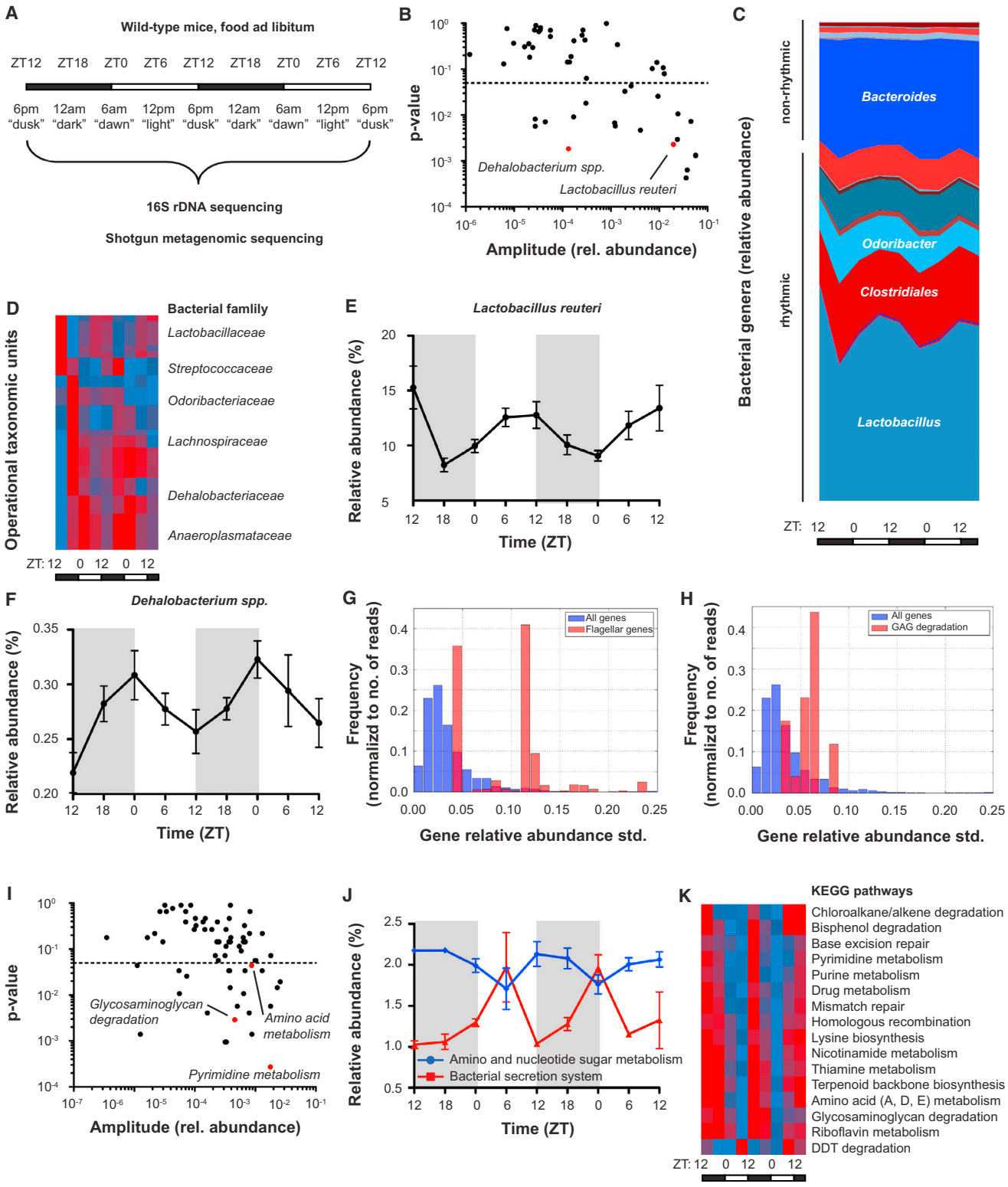

Figure 1. Intestinal Microbiota Exerts Diurnal Oscillations

(A) Schematic showing sampling times of microbiota over the course of two light-dark cycles.

(B) OTUs showing diurnal oscillations. Fluctuation amplitudes are indicated. Dashed line indicates $p < 0.05$, JTK_cycle; n = 10 individual mice at each time point.

(C) Taxonomic composition of fecal microbiota over the course of 48 hr.

(legend continued on next page)

2011). In addition to transcriptional regulation, the bacterial clock is regulated at the posttranscriptional level. Rhythmic phosphorylation of proteins in a 24 hr rhythm functions as an oscillatory system, anticipating day-night variations in environmental conditions (Johnson et al., 2008; Rust et al., 2007). It remains unknown, however, whether rhythmic activity exists in complex microbial ecosystems, some of which are not directly exposed to light-dark cycles. The mammalian intestinal microbiota constitutes such an ecosystem, whose microbial members outnumber the amount of eukaryotic cells of the host by a factor of 10. The resultant human ''metaorganism'' comprises both a eukaryotic and a prokaryotic component (Gordon, 2012; Human Microbiome Project Consortium, 2012). The microbiota plays a pivotal role in the regulation of many physiological processes, including digestion of food components, host metabolism, the maturation and function of the immune system, and even host behavior and cognitive function (Clemente et al., 2012; Hooper et al., 2012; Hsiao et al., 2013; Sommer and Bäckhed, 2013), all of which show features of circadian control. Recently, rhythmic microbial sensing by intestinal epithelial cells was found to be essential for epithelial homeostasis (Mukherji et al., 2013).

Here, we demonstrate that the gut microbiota itself follows diurnal oscillations in composition and function whose regulation is governed by host feeding rhythms. Furthermore, we find evidence in both mice and humans that host circadian misalignment results in microbial dysbiosis, which drives metabolic imbalances, suggesting an involvement of transkingdom interactions between mammalian and prokaryotic diurnal rhythms in modern human disease.

RESULTS

The Intestinal Microbiota Exhibits Diurnal Oscillations

To determine the longitudinal changes of microbiota composition over the course of a day, we performed taxonomic analysis of fecal microbiota from mice every 6 hr for two light-dark cycles (Figure 1A). All mice were fed ad libitum and housed under strict 24 hr dark-light conditions, with lights being kept on for 12 hr. Samples were taken at the time points of changing light conditions (Zeitgeber times [ZT] 12 and 0, i.e., ''dusk'' and ''dawn,'' respectively) and at the midpoint of the dark and light phases (ZT 18 and 6, respectively). We employed the commonly used nonparametric algorithm JTK_cycle to detect rhythmic elements in the taxonomic data set (Hughes et al., 2010). We detected significant ($p < 0.05$) diurnal fluctuations in the abundance of more than 15% of all bacterial operational taxonomic units (OTUs) (Figure 1B and Table S1 available online). Groups of fluctuating bacteria featured distinctive acrophase and bathyphase times with a 24 hr period. Bacterial genera rhythmically oscillating in a 24 hr cycle belonged to abundant taxonomical orders, namely Clostridiales, Lactobacillales, and Bacteroidales, such that rhythmically oscillating OTUs accounted for about 60% of the microbiota composition and resulted in time-of-day-specific taxonomic configurations (Figures 1C and 1D). Highly robust circadian fluctuations were found, for instance, in *Lactobacillus reuteri* and *Dehalobacterium spp.* (Figures 1E and 1F). The rhythmicity was reproducible regardless of housing conditions or cage effects (data not shown). We confirmed these results with a finer sampling resolution over a longer sampling period, with fecal samples being collected every 4 hr for 4 consecutive days (Figures S1A–S1D).

We next analyzed whether these diurnal oscillations in microbiota composition have consequences for the functional capacities of the intestinal microbial community over the course of a day. We therefore performed shotgun metagenomic sequencing of fecal samples collected every 6 hr over the course of two light-dark cycles and mapped the metagenomic reads to a gut microbial gene catalog (Qin et al., 2010). Although the majority of genes showed a stable level over the course of a day, certain groups of genes (such as genes involved in flagellar assembly and glycosaminoglycan degradation; Figures 1G and 1H) featured a stronger variation in abundance. To test whether such fluctuations in genes belonging to functional entities follow diurnal rhythms, we grouped genes into KEGG pathways (Kanehisa and Goto, 2000; Kanehisa et al., 2014) and employed the JTK_cycle algorithm to detect oscillations that occur with a 24 hr rhythm. Interestingly, 23% of all pathways with gene coverage above 0.2 featured diurnal rhythmicity (Figure 1I and Table S1). Among these were pathways involved in nucleotide metabolism (Figure S1E), amino acid metabolism (Figure S1F), and mucus degradation (Figure S1G). These results suggest the existence of time-of-day-specific profiles of microbiota functionality. Interestingly, it appeared that distinct functional groups exhibited coordinated antiphasic fluctuations (Figure 1J). For instance, functions involved in energy metabolism, DNA repair, and cell growth were favorably performed during the dark phase (Figure 1K), whereas the light phase featured higher abundance of ''maintenance'' pathways involved in detoxification, motility, and environmental sensing. For instance, genes performing functions in flagellar assembly, bacterial chemotaxis, and type III secretion were most abundant during the light phase (Figure S1H).

Together, these results uncover fluctuations in microbiota composition and function on the scale of hours, which follow

(D) Heatmap representation of the most significantly oscillating bacterial OTUs, JTK_cycle. Common bacterial families are listed.
(E and F) Representative examples of diurnal oscillations in the abundance of microbiota members; n = 10 mice at each time point.
(G and H) Histogram showing the distribution of daily variation in gene occurrence of flagellar genes (G) and glycosaminoglycan (GAG) degradation genes (H) versus other genes, normalized to the number of reads mapped to each gene.
(I) KEGG pathways showing diurnal oscillations. Only pathways with gene coverage > 0.2 are shown. Dashed line indicates $p < 0.05$, JTK_cycle; n = 2 individual mice at each time point.
(J) Representative examples of antiphasic diurnal oscillations in the abundance of functional KEGG pathways; n = 2 individual mice at each time point.
(K) Heatmap representation of the 16 most significantly oscillating KEGG pathways, as identified by JTK_cycle.
All p values are Bonferroni adjusted. The results shown are representative of four experiments (A–F) or two experiments (G–K). Data are expressed as mean ± SEM. See also Figure S1 and Table S1.

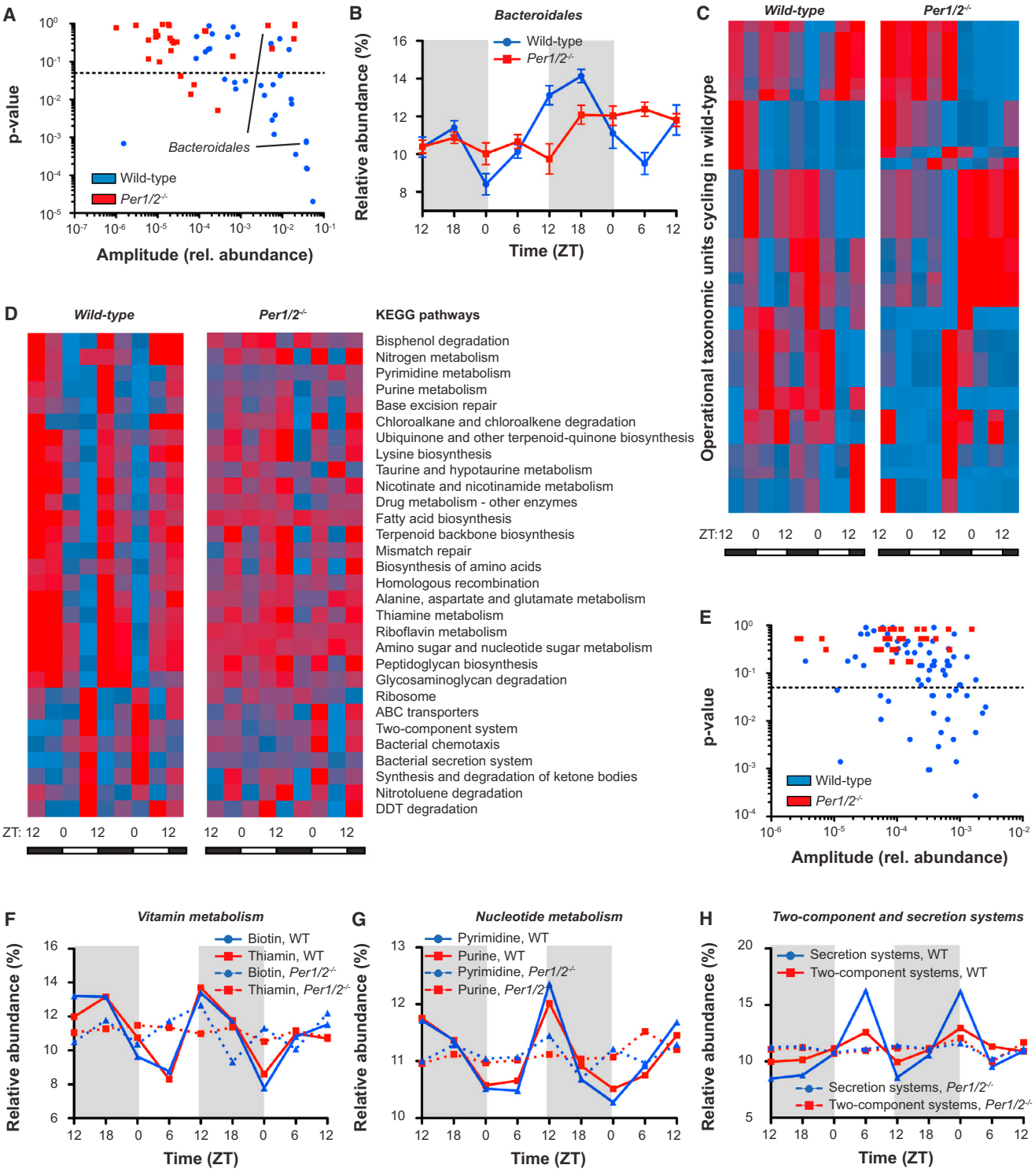

Figure 2. Loss of Diurnal Microbiota Rhythms in *Per1/2*-Deficient Mice

(A) OTUs showing diurnal oscillations in ad-libitum-fed wild-type and *Per1/2*-deficient mice. Dashed line indicates $p < 0.05$, JTK_cycle; n = 10 individual mice in each group at each time point.

(B) Representative example of OTU diurnal oscillations in wild-type mice, which are absent in *Per1/2*-deficient mice; n = 10 mice at each time point.

(C) Heatmap representation of bacterial genera oscillating with $p < 0.05$, JTK_cycle, in wild-type mice compared to *Per1/2*-deficient mice; n = 10 mice at each time point.

(legend continued on next page)

24 hr rhythmicity and which result in robust oscillations and time-of-day-specific configurations.

A Functional Circadian Clock of the Host Is Required for Diurnal Microbiota Oscillations

The observed gut microbiota diurnal rhythmicity was present despite the lack of direct microbial exposure to environmental light-dark alterations. We thus sought to determine how these rhythmic fluctuations in microbiota composition are generated in a 24 hr period. The biological clock of the host is synchronized to environmental day-night variations by the molecular components of the circadian clock. To test whether the circadian clock of the host is required for diurnal rhythmicity in microbiota composition, we used *Per1/2*$^{-/-}$ mice, which are deficient in a functional host clock (Adamovich et al., 2014). We performed a taxonomic comparison between the microbiota of wild-type and *Per1/2*$^{-/-}$ mice at each phase of the dark-light cycle over 48 hr and then used the JTK_cycle algorithm to identify rhythmic elements. Notably, *Per1/2*$^{-/-}$ mice demonstrated a near-complete loss of rhythmic fluctuations in commensal bacterial abundance (Figure 2A and Table S2), as exemplified by Bacteroidales (Figure 2B). The rhythmic pattern observed in wild-type mice was replaced by a random abundance fluctuation in clock-deficient mice with a reduction in the number of diurnally oscillating bacterial taxonomic units (Figure 2C).

To determine whether the loss of compositional oscillations has any consequences for the diurnal metagenomic profile, we performed shotgun sequencing of microbiota from *Per1/2*$^{-/-}$ mice and compared the results to wild-type mice at each phase of the day. The diurnal patterns in metagenomic pathways observed in wild-type mice were nonexistent in *Per1/2*-deficient mice (Figures 2D and 2E) and were instead replaced by mostly invariant levels of pathway activity throughout the light-dark cycle (Table S2). The preferential activity of certain functionalities during the light or dark phase was therefore lost in *Per1/2*$^{-/-}$ mice. For instance, pathways involved in vitamin metabolism (Figure 2F), nucleotide metabolism (Figure 2G), two-component and secretion systems (Figure 2H), DNA repair (Figure S2A), cell wall synthesis (Figure S2B), and motility (Figure S2C) lost their diurnal rhythmicity in *Per1/2*$^{-/-}$ mice. Together, these data indicate that a functional circadian clock of the host is required for the generation of diurnal fluctuations in the composition and function of the intestinal microbiota.

Importantly, we also noted dysbiosis in *Per1/2*-deficient mice, as evident from lower alpha diversity (Figure S2D) and distinct intestinal community composition when compared to controls (Figure S2E). Some of the biggest differences in microbiota composition between wild-type and *Per1/2*-deficient mice were found in bacterial genera, which undergo diurnal fluctuations in wild-type mice (Figure S2F). To rule out the possibility that dysbiosis and loss of diurnal microbiota oscillations are inherently connected, we analyzed other genetically modified, dysbiotic mice and tested for the existence of diurnal microbiota oscillations. We chose mice deficient in the inflammasome adaptor ASC, a model that has recently been described to feature a functionally important and well-defined dysbiosis (Elinav et al., 2011; Henao-Mejia et al., 2012). Indeed, fecal communities of wild-type and *ASC*$^{-/-}$ mice differed by alpha and beta diversity (Figures S2G and S2H). Nonetheless, bacterial OTUs from *ASC*$^{-/-}$ mice displayed significant compositional oscillations, as identified by JTK_cycle (Figures S2I and S2J). We conclude that microbiota diurnal oscillations are present at different microbiota configurations and that compositional dysbiosis and loss of diurnal rhythmicity may occur independently of each other.

Microbiota Diurnal Oscillations Are Controlled by Feeding Time

We next set out to determine the mechanism by which the circadian clock of the host is involved in generating microbial compositional oscillations in the intestine. The host circadian clock controls the rhythmicity of many physiological functions, including food consumption (Turek et al., 2005). Conversely, feeding times are central in entraining and synchronizing peripheral clocks (Asher et al., 2010; Hoogerwerf et al., 2007; Stokkan et al., 2001). Rodents are nocturnal animals that eat preferentially during the dark phase (Figure S2K). In contrast, *Per1/2*$^{-/-}$ mice feature a greatly attenuated diurnal feeding rhythm and consume food continuously throughout the day (Figure S2L). It was therefore plausible that microbiota rhythmicity in a normal wild-type host was driven by its diurnal eating habits, whereas the diminished microbiota rhythmicity in *Per1/2*$^{-/-}$ mice was secondary to its profoundly altered food consumption timing. To this end, we performed a timed feeding experiment in which wild-type mice were given access to food only during the light phase or only during the dark phase (Figures 3A, S3A, and S3B). In line with the ability of scheduled feeding to entrain peripheral clocks, this reversal of feeding habits inverted the expression pattern of intestinal clock genes (Figure S3C). After 2 weeks of continuous scheduled feeding, we collected fecal microbiota samples every 6 hr for two consecutive light-dark cycles. Using the JTK_cycle algorithm, we found that microbiota oscillations in the dark-phase-fed group were similar to ad-libitum-fed mice, reflecting the normal mainly nocturnal feeding habits of rodents (Figures 3C–3F and S3D and Table S3). In contrast, cycling OTUs often featured distinct phases between dark-phase-fed and light-phase-fed groups (Figures 3C–3F and S3D). Most cycling OTUs appeared to exhibit a phase shift of about 12 hr upon modification of feeding times, suggesting direct control of microbiota rhythms by feeding times. Such a phase shift was, for

(D) Heatmap representation of diurnal fluctuations of KEGG pathways in microbiota from wild-type mice, which are absent in microbiota from *Per1/2*-deficient mice; metagenomics analysis was performed in a total of three mice at each time point and only pathways with a coverage > 0.2 were compared.
(E) KEGG pathways showing diurnal oscillations in wild-type compared to *Per1/2*-deficient mice. Only pathways with gene coverage > 0.2 are shown. Dashed line indicates $p < 0.05$, JTK_cycle.
(F–H) Diurnal variations in genes belonging to the indicated functional pathways in wild-type and *Per1/2*-deficient mice. Metagenomics analysis was performed in a total of three mice at each time point.
The results shown are representative of two experiments. Data are expressed as mean ± SEM. See also Figure S2 and Table S2.

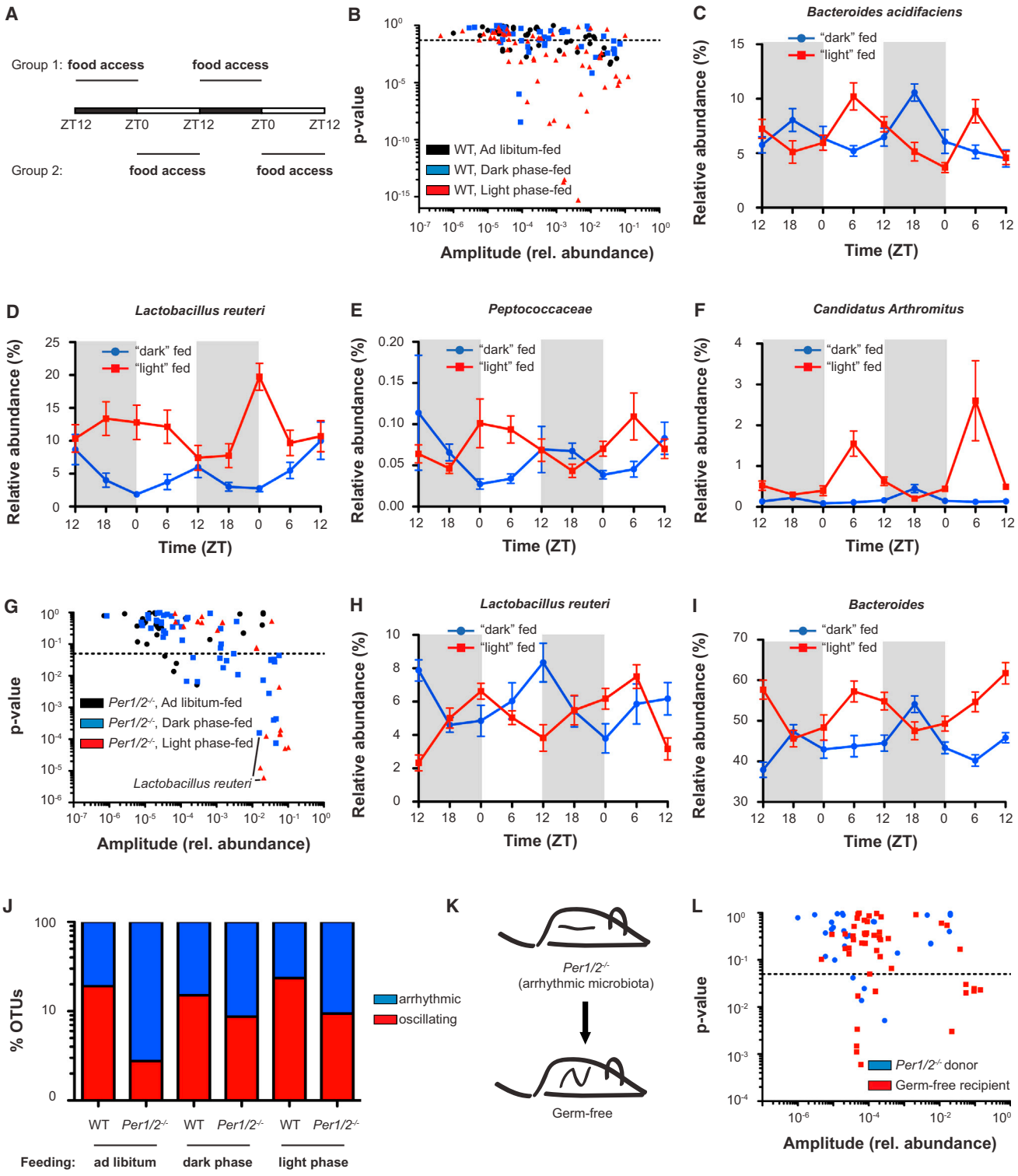

Figure 3. Feeding Rhythms Direct Diurnal Microbiota Oscillations

(A) Schematic showing timed feeding protocol. Scheduled feeding was performed for 2 weeks before sample collection.

(B) OTUs showing diurnal oscillations in wild-type mice on different feeding schedules. Dashed line indicates $p < 0.05$, JTK_cycle; n = 10 individual mice at each time point.

(C–F) Representative examples of phase shift in bacterial oscillations between dark-phase-fed and light-phase-fed wild-type mice; n = 10 mice at each time point.

(legend continued on next page)

instance, observed in the case of *Bacteroides acidifaciens* (Figure 3C), *Lactobacillus reuteri* (Figure 3D), and *Peptococcaceae* (Figure 3E). We also observed cases of de novo or enhanced rhythmicity in the light-phase-fed groups, as exemplified by *Candidatus Arthromitus* (Figure 3F). These results suggest that feeding times influence daily fluctuations in microbiota composition and that the oscillations in abundance of commensal bacteria can be controlled by scheduled feeding.

Consequently, if feeding times are directly controlling diurnal fluctuations in microbiota composition, then timed feeding should rescue the loss of such fluctuations in mice deficient in the circadian clock. We therefore performed a similar food restriction experiment on *Per1/2*$^{-/-}$ mice and analyzed microbiota samples every 6 hr over two light-dark cycles after 2 weeks of scheduled feeding. Indeed, both light-phase-fed and dark-phase-fed, but not ad-libitum-fed, *Per1/2*$^{-/-}$ mice featured significantly oscillating bacterial OTUs, demonstrating de novo rhythmicity generation in a formerly arrhythmic community composition (Figures 3G and S3E and Table S3). Similar to wild-type mice undergoing timed feeding, the phase of microbiota oscillations followed the feeding time in *Per1/2*$^{-/-}$ mice, and oscillating OTUs showed phase shifts between dark-phase-fed and light-phase-fed mice (Figure S3E). For instance, the oscillations in *Lactobacillus reuteri* (Figure 3H) and *Bacteroides* (Figure 3I) observed in dark-phase-fed *Per1/2*$^{-/-}$ mice followed the patterns observed in ad-libitum-fed or dark-phase-fed wild-type mice, whereas the light-phase-fed group exhibited opposite cycles. These results demonstrate that rhythmic feeding can reconstitute OTU oscillations in *Per1/2*$^{-/-}$ mice (Figure 3J).

To further corroborate the centrality of host feeding rhythmicity in controlling microbiota oscillations, we transplanted microbiota from *Per1/2*$^{-/-}$ mice (lacking diurnal fluctuations) into wild-type germ-free mice that were housed under normal light-dark conditions (Figure 3K). Upon fecal transplantation, colonized germ-free mice exhibited regular nocturnal activity and metabolic patterns (Figures S3F and S3G). This was also observed when control transplantations with microbiota from wild-type mice were performed (Figure S3H). One week after transplantation into the germ-free host, fecal microbiota from *Per1/2*$^{-/-}$ mice featured a normalized diurnal rhythmicity (Figure 3L).

Taken together, our results show that rhythmicity of food intake dictates daily oscillations in microbiota composition and that microbiota rhythmicity is a flexible process that can be lost or regained in response to changed feeding behaviors. Thus, feeding times couple the circadian patterns of host behavior to diurnal fluctuations in microbiota composition and function.

Environmental Disruption of Normal Sleep Patterns Induces Loss of Microbiota Diurnal Rhythmicity and Dysbiosis

We next sought to test the physiological relevance of microbiota diurnal rhythmicity. In humans, disturbances of the circadian clock often occur in the setting of shift work and chronic jet lag, where external light conditions change frequently and impair the ability of the molecular clock to adapt to a stable rhythm. We mimicked this situation in mice by using a jet lag model in which mice were exposed to an 8 hr time shift every 3 days (Figure 4A). To this end, mice were subjected to an 8 hr light cycle advance, remained under these conditions for 3 days, and were then reverted back to the original light-dark cycle. After another 3 days, this pattern was repeated. This model simulates the jet lag situation induced by frequent flying between countries with an 8 hr time difference and likewise mimics a scenario of regular switching between day and night shift work (Huang et al., 2011; Yamaguchi et al., 2013). After 4 weeks of jet lag induction, mice returned to the starting light cycle conditions and were analyzed 1 day after the last time shift. Induction of jet lag resulted in the loss of host rhythmic physical activity (Figures S4A and S4B). Similar to humans, jet lag also led to an irregular pattern of food intake rhythms, resulting in a loss of day-night variations in food consumption (Figures 4B and S4C). Nonetheless, the overall daily amount of food intake was not affected between control and jet-lagged mice (Figure 4B). Successful induction of jet lag was also confirmed by a shift in peripheral clock transcript oscillations (Figures S4D–S4F).

Given our finding that rhythmic food intake induces diurnal fluctuations in the microbiota, we examined whether these disruptions of rhythmic behavior by jet lag would also impair diurnal oscillations in microbiota composition. To this end, we performed a taxonomic analysis of microbiota composition every 6 hr in jet-lagged mice and tested for rhythmicity by JTK_cycle. Analogous to mice deficient in the circadian clock, jet-lagged mice featured an abrogation of bacterial rhythms with a reduced number of oscillating bacterial taxonomic units (Figures 4C–4E; see also Table S4). Together, similar to genetic disruption of the circadian clock, environmentally induced abrogation of daily oscillatory patterns was associated with loss of diurnal rhythmicity in microbiota composition.

Our observation of dysbiosis in genetically clock-deficient mice prompted us to analyze the community composition of ''jet-lagged'' mice after 4 weeks of time shifts. Indeed, microbiota composition slightly differed between control and jet lagged mice (Figure 4F). When we followed mice for a period of 16 weeks of continuous time shifting, dysbiosis was enhanced

(G) OTUs showing diurnal oscillations in *Per1/2*-deficient mice on different feeding schedules. Dashed line indicates $p < 0.05$, JTK_cycle; n = 10 individual mice at each time point.

(H and I) Representative examples of phase shift in bacterial oscillations between dark-phase-fed and light-phase-fed *Per1/2*-deficient mice; n = 10 mice at each time point.

(J) Quantification of oscillating OTUs with $p < 0.05$, JTK_cycle, in wild-type and *Per1/2*-deficient mice on different feeding schedules.

(K) Schematic showing fecal transplantation of microbiota from *Per1/2*-deficient mice (arrhythmic microbiota) into germ-free recipients (gain of rhythmicity).

(L) OTUs showing diurnal oscillations in microbiota from *Per1/2*-deficient mice before and after transplantation into wild-type germ-free mice. Dashed line indicates $p < 0.05$, JTK_cycle; n = 10 individual mice at each time point in each group.

The results are representative of two independent experiments. Data are expressed as mean ± SEM. See also Figure S3 and Table S3.

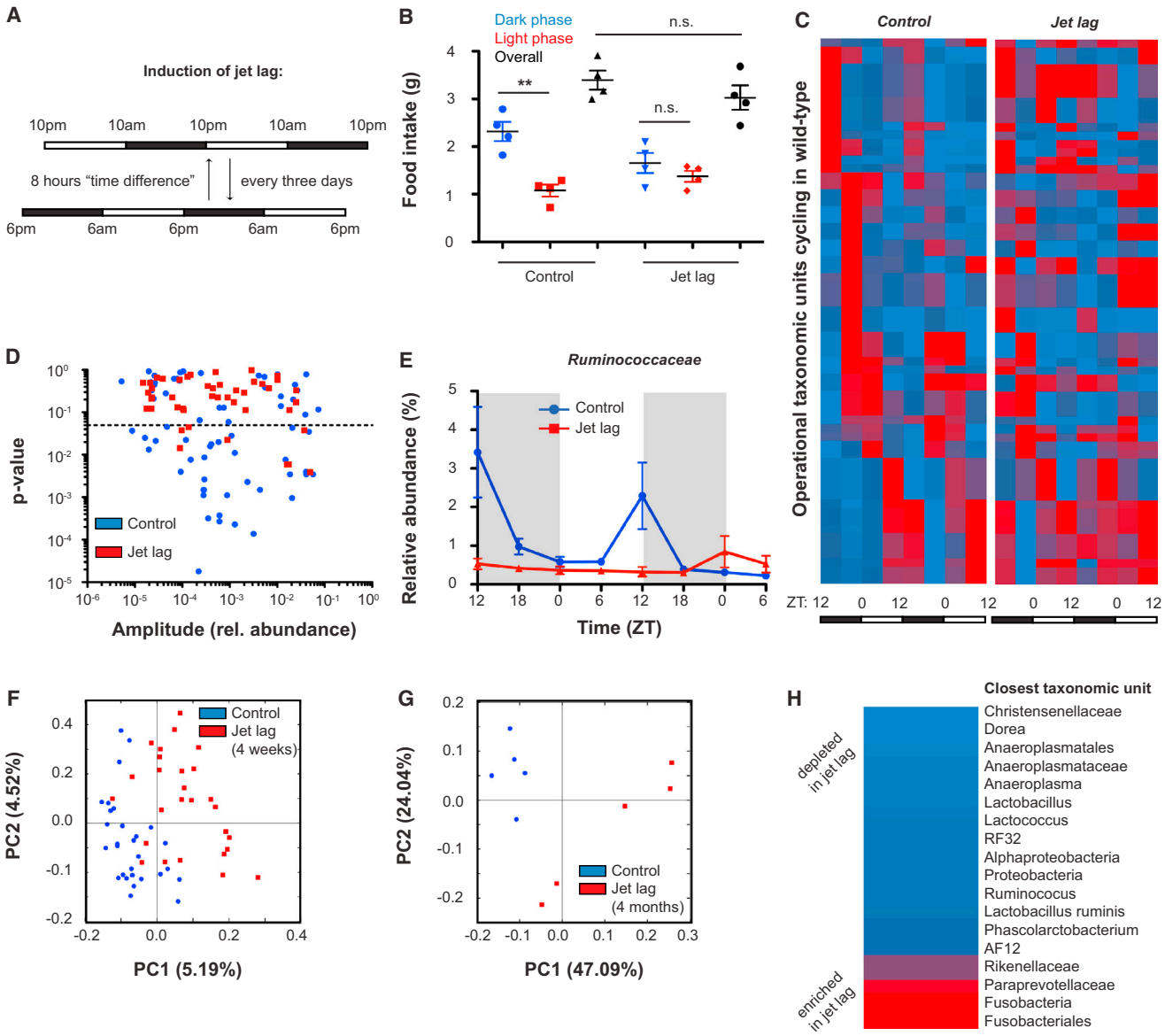

Figure 4. Jet Lag Leads to Loss of Diurnal Microbiota Oscillations and Dysbiosis

(A) Schematic showing induction of jet lag by constant time shifting by 8 hr. Every 3 days, mice were subjected to a forward or backward shift of 8 hr. Controls remained under constant light-dark cycle conditions.

(B) Food intake of control and jet lag mice during the dark phase, light phase, and combined. **$p < 0.01$, n.s. not significant.

(C) Heatmap representation of bacterial genera oscillating with $p < 0.05$, JTK_cycle, in control mice compared to jet-lagged mice; n = 5 mice at each time point.

(D) OTUs showing diurnal oscillations in control and jet lag mice. Dashed line indicates $p < 0.05$, JTK_cycle; n = 5 individual mice at each time point.

(E) Representative example of bacterial oscillations in wild-type mice, which are lost under jet lag; n = 5 mice at each time point.

(F) Beta diversity of gut microbial communities in control and jet lag mice after 4 weeks of time shifts. Samples are pooled from different times of the day.

(G) Beta diversity of gut microbial communities in control and jet lag mice after 4 months of time shifts.

(H) Heatmap representation of changes in microbial composition induced by jet lag.

Data are expressed as mean ± SEM. See also Figure S4 and Table S4.

(Figure 4G) and partially affected taxonomic units that were found to be oscillating in wild-type mice (Figure 4H and Table S4). Altogether, these data suggest that chronic environmental or genetic disruption of the mammalian dark-light cycle manifests as significant alterations in feeding rhythms and as a failure to maintain microbiota rhythmicity and composition.

Dysbiosis Associated with Environmental Clock Disruption Drives Metabolic Disease

Chronic jet lag and shift work are behavioral patterns that have become widespread in humans only recently, following the industrial revolution. These newly introduced behavioral patterns are associated with increased risk for obesity, diabetes, and

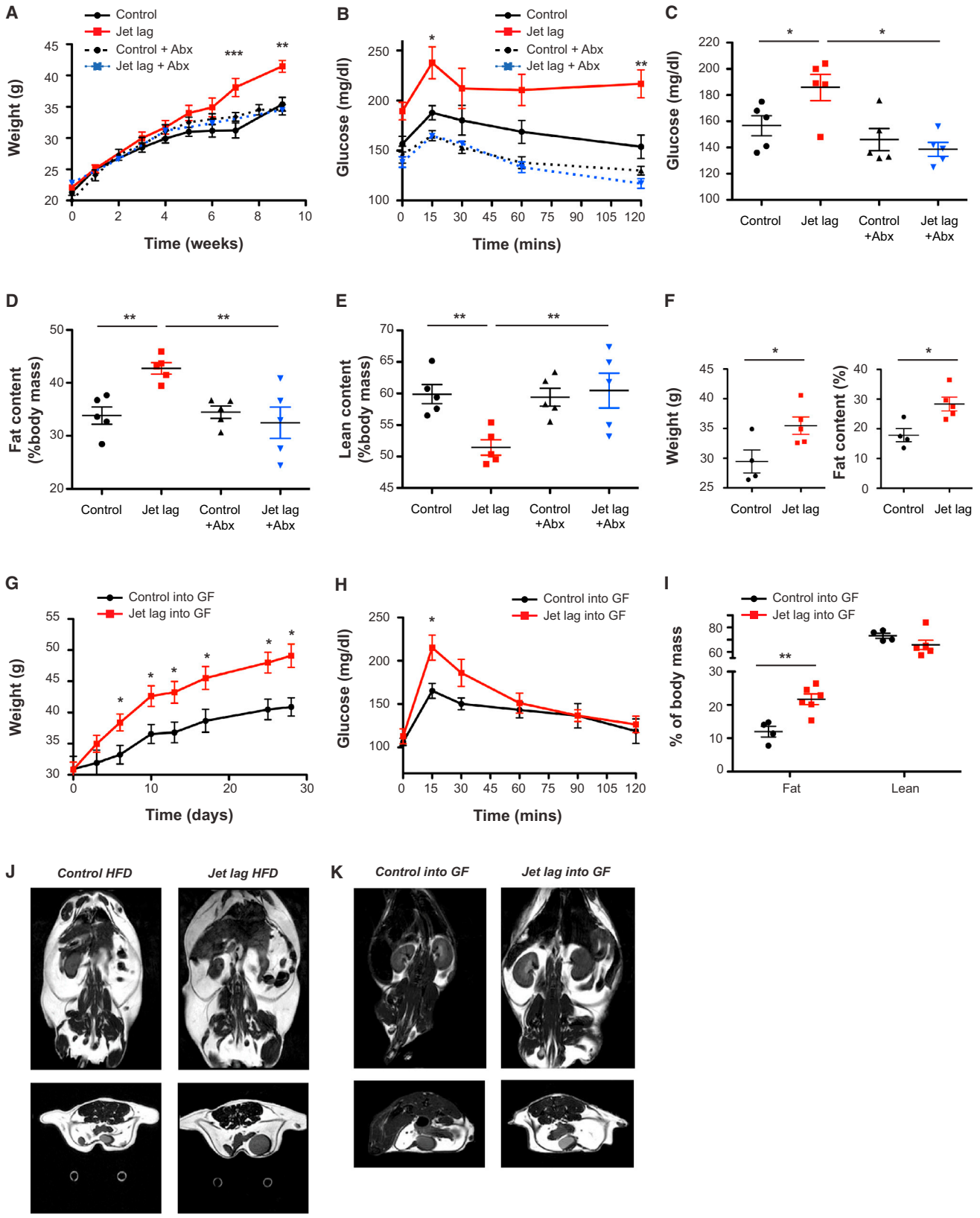

(legend on next page)

cardiovascular disease, all disease states that have emerged in parallel in modern human populations (Archer et al., 2014; Buxton et al., 2012; Fonken et al., 2010; Scheer et al., 2009; Suwazono et al., 2008). Because we found loss of microbiota oscillations and dysbiosis to be associated with jet lag in mice, we set out to test whether the microbiota is involved in metabolic imbalances associated with altered circadian rhythms. We first established that jet lag is linked to manifestations of the metabolic syndrome. We fed jet-lagged and control mice a high-fat diet, containing 60% of caloric energy from fat, thereby mimicking human dietary habits predisposing to the metabolic syndrome. Indeed, as early as 6 weeks after instating of high-fat diet, time-shifted mice exhibited enhanced weight gain and exacerbated glucose intolerance as compared to mice maintained on normal circadian rhythmicity (Figures 5A–5C). Because the overall food intake was not different between wild-type and jet-lagged mice (Figure 4B), we hypothesized that alterations in microbiota composition may contribute to this metabolic phenotype. Indeed, wide-spectrum antibiotic treatment for the duration of jet lag induction (vancomycin, ampicillin, kanamycin, and metronidazole; Fagarasan et al., 2002; Rakoff-Nahoum et al., 2004) abrogated obesity and glucose intolerance in jet-lagged mice (Figures 5A–5C). Obesity in time-shifted mice was associated with higher fat mass, which was rescued by antibiotic treatment (Figures 5D and 5E). MRI revealed that this accumulation of fat mass resulted in increased subcutaneous and visceral fat deposition in mice that underwent chronic time shifting (Figure 5J).

Of note, glucose tolerance by itself underlies circadian variation (Kaasik et al., 2013; So et al., 2009). Nevertheless, diurnal differences in glucose intolerance between jet-lagged and control groups persisted irrespective of daily time of measurement (data not shown). Disruption of nocturnal behavior and feeding patterns in jet-lagged mice was unaffected by high-fat diet or antibiotics treatment (Figures S5A–S5F). Although high-fat feeding did reduce, to some extent, the number of oscillating OTUs (Figures S5G–S5I and Table S5), microbiota oscillations persisted after 1 week of antibiotics treatment (Figures S5J–S5L and Table S5). Moreover, jet-lagged mice maintained on regular chow diet for 4 months also featured higher body weight and increased body fat mass as compared to their non-jet-lagged controls (Figure 5F), highlighting the fact that jet-lag-induced adverse metabolic effects were independent of the dietary composition.

To further corroborate the role of the altered microbiota in the metabolic imbalances observed in jet-lagged mice, we performed fecal transfer of control or "jet-lagged" microbiota configurations into germ-free Swiss Webster mice. Recipients of the time-shifted microbiota exhibited enhanced weight gain and glucose intolerance as compared to control microbiota recipients (Figures 5G and 5H). Furthermore, similar to their respective donors, recipients of microbiota from time-shifted mice featured a significant increase in body adiposity (Figure 5I). MRI scanning showed an increase in body fat in germ-free mice that had received microbiota from jet-lagged donors (Figure 5K). Collectively, these results demonstrate that jet-lag-associated metabolic derangements are transmissible by the microbiota.

Human Microbiota Exhibits Diurnal Oscillations and Time-Shift-Associated Dysbiosis with Metabolic Consequences

Finally, we examined whether our findings in animal models may apply to humans. We first determined microbiota community variations in human fecal samples from two subjects collected at multiple time points during the day for several consecutive days (Figure 6A and Table S6). Using 16S rDNA sequencing, we found diurnal fluctuations in the abundance of up to 10% of all bacterial OTUs (Figures 6B and 6C). Similar to what we had documented in mice, oscillating OTUs feature distinct acrophases and bathyphases over the course of a day (Figure 6D). Robust oscillations were found, for instance, in *Parabacteroides* (Figure 6E), *Lachnospira* (Figure S6A), and *Bulleida* (Figure S6B). The diurnal rhythmicity in OTU abundance resulted in time-of-day-specific microbiota community configurations with a repetitive pattern over the observed time period (Figure S6C). We also performed metagenomic analysis of human samples at multiple times of a day and found that about 20% of all pathways with a gene coverage higher than 0.2 exhibited a diurnal abundance pattern (Figures 6F), as exemplified by genes belonging to dioxin degradation pathways (Figure S6D). Analogous to our findings in mice, distinct functional entities featured preferential abundance at different times of the day. For example, energy metabolism and protein production were preferentially performed during the light phase, whereas detoxification pathways were mostly active during the night (Figures 6G and 6H). The peak phases of pathway activity occurred at opposite times of the day

Figure 5. Jet-Lag-Induced Dysbiosis Promotes Metabolic Derangements

(A–E) Mice underwent time-shift-induced jet lag and were fed a high-fat diet. Half of the mice were treated with antibiotics (Abx); n = 10 mice in each group.
(A) Weight gain over 9 weeks of high-fat feeding. $^{**}p < 0.01$ and $^{***}p < 0.001$.
(B) Oral glucose tolerance test performed 8 weeks after initiation of jet lag. $^{*}p < 0.05$ and $^{**}p < 0.01$.
(C) Fasting glucose levels of control and jet lag mice, with or without Abx treatment, after 8 weeks of jet lag. $^{*}p < 0.05$.
(D and E) Fat (D) and lean (E) body mass of control and jet lag mice, with or without Abx treatment, after 8 weeks of jet lag. $^{**}p < 0.01$.
(F) Weight and fat content of control and jet lag mice after 4 months of time shifts in the jet lag group. $^{*}p < 0.05$.
(G–I) Microbiota from control or jet lag mice was transplanted into germ-free (GF) mice; n = 4–6 mice in each group.
(G) Weight gain over 4 weeks. $^{*}p < 0.05$.
(H) Oral glucose tolerance test performed on day 3 post fecal transfer. $^{*}p < 0.05$.
(I) Fat and lean body mass in recipient mice one month post fecal transfer. $^{**}p < 0.01$.
(J) T_2-weighted MR images of control and jet lag mice after 8 weeks of jet lag. Above, coronal images; below, axial images.
(K) T_2-weighted MR images of recipient mice 1 month post fecal transfer. Above, coronal images; below, axial images.
The results shown are representative of three (A–E) and two (G–I) independent experiments.
Data are expressed as mean ± SEM. See also Figure S5 and Table S5.

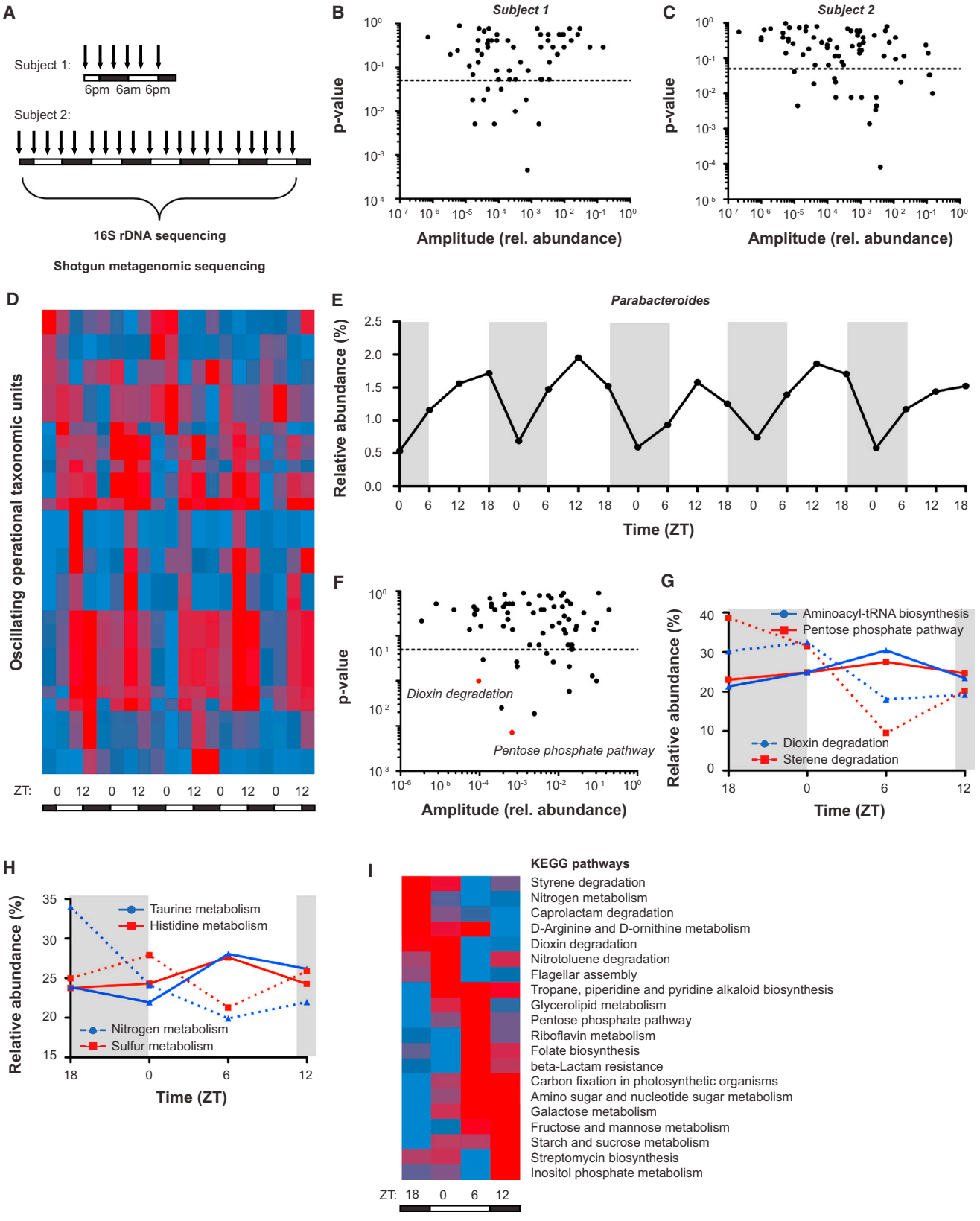

(legend on next page)

compared to mouse microbiota (Figure 6I), as would be expected from diurnal versus nocturnal behavior of the host. Together, these data suggest that, like in mice, components of the human intestinal microbiota may undergo diurnal variations in composition and function.

Furthermore, our data in mice suggest that disruption of the circadian clock by aberrant sleep-activity cycles leads to aberrant microbiota composition. The time shift model we applied in mice corresponds to the jet lag induced by flying between countries with an 8 hr time difference. We therefore collected fecal samples from two healthy human donors who underwent such a flight-induced time shift of 8 to 10 hr (flying from central or western United States time zones to Israel) and performed a taxonomic analysis 1 day before the induction of travel-induced jet lag, during jet lag (1 day after landing), and after recovery from jet lag (2 weeks after landing) (Figure 7A). Indeed, microbiota communities showed a time-shift-induced change in composition, detected 24 hr into jet lag (Figure 7B and Table S7). Microbiota samples obtained during jet lag showed a higher relative representation of Firmicutes, which was reversed upon recovery from jet lag. Interestingly, Firmicutes have been associated with a higher propensity for obesity and metabolic disease in multiple human studies (Ley et al., 2006; Ridaura et al., 2013). To analyze whether the microbiota changes in jet-lagged individuals were associated with increased susceptibility to metabolic disease, we performed fecal transfer experiments into germ-free mice of human samples obtained from individual subjects before jet lag, 24 hr into jet lag, and following recovery from jet lag (Figure 7C). Germ-free mice colonized with microbiota from jet-lagged individuals displayed enhanced weight gain and featured higher blood glucose levels after oral glucose challenge compared to samples taken before the time shift (Figures 7D and 7E). This metabolic alteration was reversed following recovery from jet lag (Figures 7D and 7E). Furthermore, germ-free recipients of microbiota from the jet-lagged state accumulated more body fat than mice receiving microbiota from the same subjects before or after jet lag (Figure 7F). Together, albeit preliminary, these data suggest that members of the human microbiota undergo diurnal oscillations, that circadian misalignment in humans is associated with dysbiosis, and that the resulting microbial community may contribute to metabolic imbalances.

DISCUSSION

In this study, we describe that the mammalian gut microbiota displays diurnal oscillations, which are governed by food consumption rhythmicity. If rhythmic feeding times are distorted, as in the case of genetic clock deficiency or time-shift-induced jet lag, then microbiota oscillations are impaired (Figure S7). Chronic circadian misalignment in mice and time-shift-induced jet lag in humans result in dysbiosis and transmissible metabolic consequences, including obesity and glucose intolerance. These observations provide the first example of how a symbiotic community may synchronize its interdependent physiologic activities to the geophysical clock and how this promotes homeostasis of the metaorganism.

Previous studies looking at temporal fluctuations in the microbiota have considered longer time frames and found a remarkable stability of individual microbial compositions over time (Faith et al., 2013; Lozupone et al., 2012). Here, we performed the longitudinal microbiota study with a finer temporal resolution and found an hour-scale fluctuation with a diurnal rhythm. Notably, our analysis focuses on the diurnal variations in microbial community composition and metagenomic pathways. Because molecular components of bacterial circadian clocks have also been described to function on the transcriptional and posttranscriptional level (Lenz and Søgaard-Andersen, 2011), it is possible that some members of the commensal microbiota harbor yet another level of time-dependent activity control, which, in addition to the patterns in relative abundance, might regulate bacterial activity in a rhythmic manner.

Our results have several implications. First, they suggest that the metabolic imbalances associated with chronic disturbances of host circadian rhythms, such as the ones found in shift workers and during jet lag, have a communicable component that depends on the composition of the microbiota and its effect on host metabolism. The morbidities associated with disruptions of host circadian rhythms are emerging diseases of the modern life style, and the underlying etiology is highly multifactorial. Our study identifies alterations in intestinal microbial communities as an additional driving force of such disease manifestations and implies that targeted probiotic or antimicrobial therapy may be tested as potential new preventive or therapeutic approaches. The results presented here may thus prompt future studies to determine the impact of circadian misalignment on factors shaping the microbiota, including immune and metabolic pathways of the host, eating patterns, stress hormone levels, and bowel movement.

Second, our study reveals that, in addition to the type of diet being a modulator of microbiota composition, the timing of food intake plays a critical role in shaping intestinal microbial ecology. When food intake is rhythmic, we found that around 15% of commensal bacterial taxonomic units (and a much higher percentage of abundance) fluctuate over the course of a day. Analogous to peripheral clocks, the microbiota rhythms are influenced by the host clock and perform critical functions in the

Figure 6. Human Microbiota Undergoes Diurnal Oscillations in Composition and Function

(A) Schematic showing approximate sampling times of human microbiota from two subjects over the course of multiple light-dark cycles.

(B and C) OTUs showing diurnal oscillations in two human subjects. Dashed line indicates $p < 0.05$, JTK_cycle.

(D) Heatmap representation of bacterial genera from one human subject oscillating with $p < 0.05$, JTK_cycle.

(E) Representative example of diurnal bacterial oscillations over 5 consecutive days.

(F) KEGG pathways showing diurnal oscillations. Only pathways with gene coverage > 0.2 are shown. Dashed line indicates $p < 0.05$, JTK_cycle.

(G and H) Examples of antiphasic abundance peaks in KEGG pathways from human microbiota. ZT data are pooled from 5 consecutive days.

(I) Heatmap Representation of Diurnal Oscillations in KEGG Pathways

See also Figure S6 and Table S6.

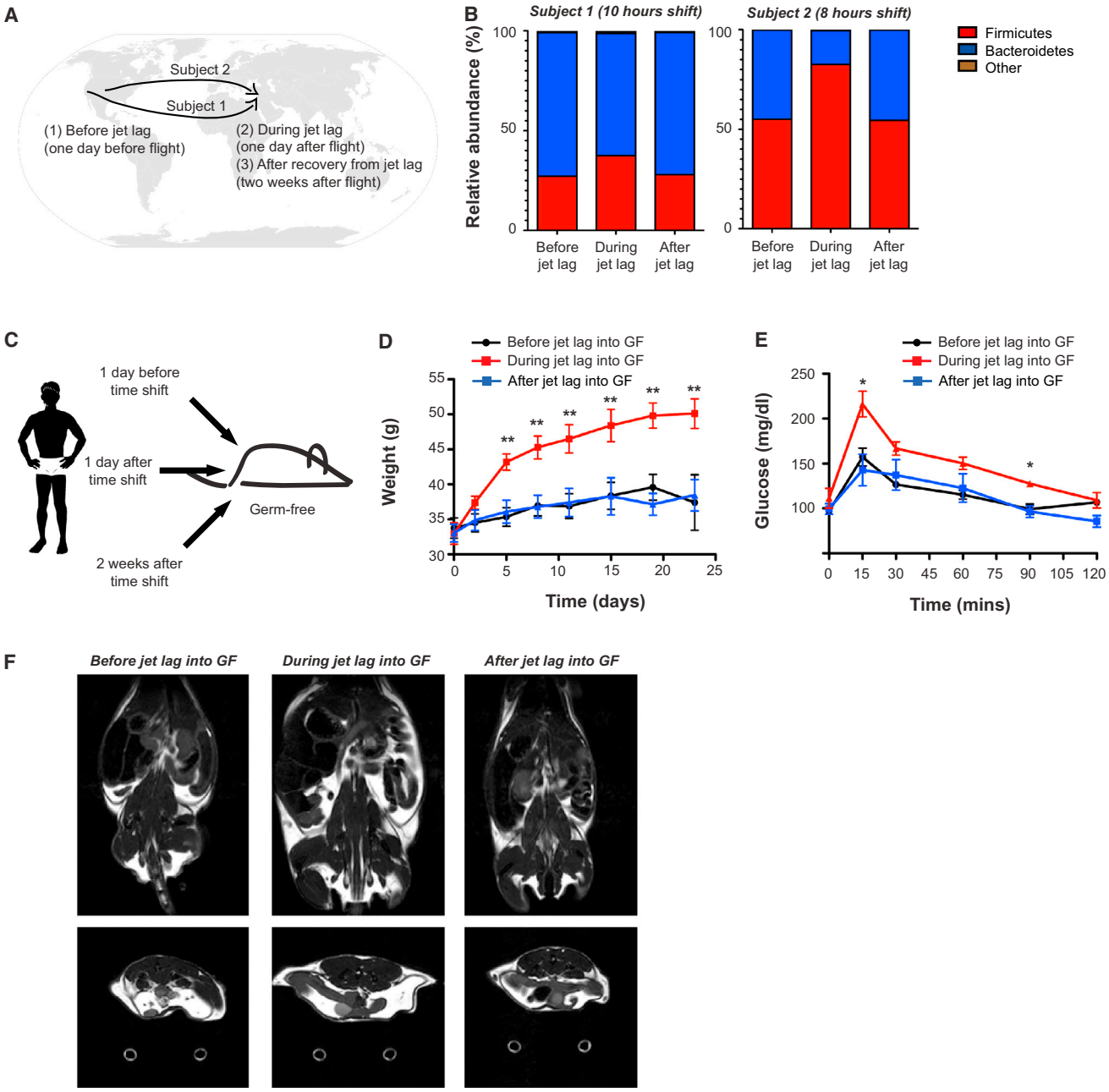

Figure 7. Jet Lag in Humans Is Associated with Dysbiosis that Drives Metabolic Derangements

(A) Schematic showing times of microbiota sampling from subjects before, during, and after jet lag induced by an 8–10 hr time shift.

(B) Phylum level composition of microbiota from two human subjects corresponding to the sampling times shown in (A).

(C) Schematic of fecal transplantation from human subjects before, during, and after jet lag into germ-free mice.

(D) Weight gain of recipient mice over 3 weeks; n = 5 mice in each group. **p < 0.01.

(E) Oral glucose tolerance test of recipient mice performed on day 3 post fecal transfer; n = 5 mice in each group. *p < 0.05.

(F) T_2-weightd MR images of recipient mice performed 3 weeks after fecal transfer. Above, coronal images; below, axial images.

The results shown are representative of two independent experiments (C–F).

Data are expressed as mean ± SEM. See also Figure S7 and Table S7.

adaptation of metabolic processes to the diurnal fluctuations in the environment. Indeed, recent work has shown that cues from the microbiota play an important role in the generation of circadian rhythms in intestinal epithelial cells (Mukherji et al., 2013). Together, this recent work and the present study suggest an emerging paradigm whereby a feedback loop exists between diurnal oscillations of the host and the microbiota with mutual cross-regulation of interdependent functions.

In addition, the diurnal fluctuations in intestinal microbial ecology discovered here should be taken into account when interpreting studies focusing on human and animal microbiota composition. Based on our results, it might be advisable that human subjects involved in microbiota studies provide their samples at a standardized time of the day in order to exclude the effect of diurnal variations on the interpretation of diet or treatment modalities. Our study reveals that dysbiosis has a temporal dimension and that static microbiota comparisons might not be fully conclusive unless samples were taken in a controlled manner with respect to this important additional variable. Short-term rhythmic oscillations in the microbiota, such as the ones described in this study, may be exaggerated or disrupted under various disease conditions, and it will be interesting to determine the impact of such "temporal dysbiosis" on microbiota-mediated diseases with different manifestations or varying degrees of severity at different phases of the day.

Finally, the network of codependent diurnal rhythms between the host and its indigenous microbiota might confer several biological advantages to the metaorganism. A dynamic microbiota composition may be able to meet the challenges imposed by diurnal fluctuations in the environment better than a temporally static composition. As demonstrated in this study, food intake by the host undergoes circadian fluctuations, which evoke temporal changes in the bacterial species involved in nutrient metabolism. Thus, oscillations in components of the microbiota might anticipate these temporal variations in nutrient availability. We found that pathways involved in growth and energy metabolism (such as nucleic acid repair, nucleotide metabolism, and carbohydrate and amino acid metabolism) are antiphasic to motility and detoxification pathways (including flagellar assembly, chemotaxis, and xenobiotics degradation). Because our taxonomic analysis indicates that microbiota oscillations are following rhythmic food intake, such metagenomic fluctuations might be the result of rhythmic niche occupation by specialists, which are responsive to phases of food intake/starvation. In such a scenario, the nonoscillating species would represent a population responsible for "housekeeping" functions that are not subject to diurnal changes. Moreover, the microbiota provides colonization resistance against foreign microbial elements, including enteric pathogens (Stecher and Hardt, 2011) that are potentially introduced by food consumption during waking hours. As such, the introduction of foreign microbial elements into the intestinal microbiota underlies daily fluctuations, generating the need for diurnal rhythmicity of niche occupation by the commensal microbiota. Unraveling the roles and regulators of diurnal microbiota oscillations may add an important facet to our quest for molecular elucidation of the principles of symbiotic coexistence of host with its microbial milieu, and modulation of microbiota rhythmicity may consequently be exploited therapeutically.

EXPERIMENTAL PROCEDURES

Mice

Mice were kept under strict light-dark cycles, with lights being turned on at 6 AM and turned off at 6 PM. For the induction of jet lag, mice were shifted between control light conditions (lights turned on at 6 AM and turned off at 6 PM) and an 8 hr time difference (lights turned on at 10 PM and turned off at 10 AM) every 3 days. Experiments performed on jet-lagged mice were done when these mice were in the same light-dark cycle as control mice, and ZTs were synchronized (i.e., ZT0 of jet lag mice corresponded to ZT0 of control mice, as all mice were exposed to the same light-dark conditions at the onset of sample collection). In food restriction experiments, mice were housed under standard light-dark conditions (6 AM to 6 PM) but had access to food only during the light or dark phase, respectively, for 2 weeks. For antibiotic treatment, mice were given a combination of vancomycin (1 g/l), ampicillin (1 g/l), kanamycin (1 g/l), and metronidazole (1 g/l) in their drinking water. Stool samples were collected fresh and on the basis of individual mice. For experiments involving gnotobiotic mice, germ-free Swiss Webster mice were housed in sterile isolators. For fecal transplantation experiments, 100 mg of stool was resuspended in 1 ml of PBS, homogenized, and filtered through a 70 μm strainer. Recipient mice were gavaged with 200 μl of the filtrate.

Microbiota Analysis

For 16S amplicon sequencing, PCR amplification was performed spanning the V1/2 region of the 16S rRNA gene and subsequently sequenced using 500 bp paired-end sequencing (Illumina MiSeq). For metagenomic shotgun analysis, libraries were sequenced using 50 bp single-read sequencing (Illumina HiSeq).

Statistical Analysis

Data are expressed as mean ± SEM. For the analysis of rhythmic oscillations and their amplitudes, the nonparametric test JTK_cycle was used (Hughes et al., 2010), incorporating a window of 18–24 hr for the determination of circadian periodicity. Bonferroni-adjusted p values < 0.05 were considered significant. The Benjamini-Hochberg procedure was used to control the false discovery rate. JTK_cycle results are provided in supplemental tables. Differences in metabolic data were analyzed by ANOVA, and post hoc analysis for multiple group comparison was performed. Pairwise comparison between host transcript data was performed using Student's t test.

A detailed description of materials and methods used in this paper can be found in the Extended Experimental Procedures.

ACCESSION NUMBERS

The European Nucleotide Archive (ENA) accession number for the microbial shotgun and 16S sequences is PRJEB7112.

SUPPLEMENTAL INFORMATION

Supplemental Information includes Extended Experimental Procedures, seven figures, and seven tables and can be found with this article online at http://dx.doi.org/10.1016/j.cell.2014.09.048.

AUTHOR CONTRIBUTIONS

C.A.T. conceived the project, designed and performed all experiments, interpreted the results, and wrote the manuscript. D.Z., G.Z.-S., J.S., T.K., and S.G. conducted computational and bioinformatics analysis. M.L., A.C.T., L.A., and M.N.K. helped with experiments. D.Z. and M.L. equally contributed to this study. Y.K. and I.B. performed metabolic cage experiments and MRI studies, respectively. N.Z. and Z.H. conducted and supervised human sample collection. A.H. supervised the germ-free mouse experiments. H.S. provided essential help with the metabolic studies. E.S. supervised the computational analysis and provided critical insight to the manuscript. E.E. conceived and directed the project, designed experiments, interpreted the results, and wrote the manuscript.

ACKNOWLEDGMENTS

We thank the members of the Elinav lab for fruitful discussions. We thank Gad Asher and Liat Rousso-Noori (Department of Biological Chemistry, Weizmann Institute of Science) for helpful advice, meaningful insights, and for providing *Per1/2*$^{-/-}$ mice. *ASC*$^{-/-}$ mice were kindly provided by Richard Flavell (Yale

University). We acknowledge Carmit Bar-Nathan for dedicated germ-free mouse care taking. We thank the Weizmann Institute management and The Nancy and Stephen Grand Israel Center for Personalized Medicine for providing financial and infrastructure support. C.A.T. is the recipient of a Boehringer Ingelheim Fonds PhD Fellowship and thanks Shalev Itzkovitz and Yair Reisner for helpful discussions. E.E. is supported by Yael and Rami Ungar, Israel; Abisch Frenkel Foundation for the Promotion of Life Sciences; the Gurwin Family Fund for Scientific Research; Leona M. and Harry B. Helmsley Charitable Trust; Crown Endowment Fund for Immunological Research; estate of Jack Gitlitz; estate of Lydia Hershkovich; the Benoziyo Endowment Fund for the Advancement of Science; Adelis Foundation; John L. and Vera Schwartz, Pacific Palisades; Alan Markovitz, Canada; Cynthia Adelson, Canada; CNRS (Centre National de la Recherche Scientifique); estate of Samuel and Alwyn J. Weber; Mr. and Mrs. Donald L. Schwarz, Sherman Oaks; grants funded by the European Research Council; the Kenneth Rainin Foundation; the German-Israel Binational foundation; the Israel Science Foundation; the Minerva Foundation; the Rising Tide foundation; and the Alon Foundation scholar award. E.E. is the incumbent of the Rina Gudinski Career Development Chair.

Received: February 20, 2014
Revised: June 27, 2014
Accepted: September 18, 2014
Published: October 16, 2014

REFERENCES

Adamovich, Y., Rousso-Noori, L., Zwighaft, Z., Neufeld-Cohen, A., Golik, M., Kraut-Cohen, J., Wang, M., Han, X., and Asher, G. (2014). Circadian clocks and feeding time regulate the oscillations and levels of hepatic triglycerides. Cell Metab. *19*, 319–330.

Archer, S.N., Laing, E.E., Möller-Levet, C.S., van der Veen, D.R., Bucca, G., Lazar, A.S., Santhi, N., Slak, A., Kabiljo, R., von Schantz, M., et al. (2014). Mistimed sleep disrupts circadian regulation of the human transcriptome. Proc. Natl. Acad. Sci. USA *111*, E682–E691.

Asher, G., Reinke, H., Altmeyer, M., Gutierrez-Arcelus, M., Hottiger, M.O., and Schibler, U. (2010). Poly(ADP-ribose) polymerase 1 participates in the phase entrainment of circadian clocks to feeding. Cell *142*, 943–953.

Bass, J. (2012). Circadian topology of metabolism. Nature *491*, 348–356.

Buxton, O.M., Cain, S.W., O'Connor, S.P., Porter, J.H., Duffy, J.F., Wang, W., Czeisler, C.A., and Shea, S.A. (2012). Adverse metabolic consequences in humans of prolonged sleep restriction combined with circadian disruption. Sci. Transl. Med. *4*, 129ra143.

Clemente, J.C., Ursell, L.K., Parfrey, L.W., and Knight, R. (2012). The impact of the gut microbiota on human health: an integrative view. Cell *148*, 1258–1270.

Dibner, C., Schibler, U., and Albrecht, U. (2010). The mammalian circadian timing system: organization and coordination of central and peripheral clocks. Annu. Rev. Physiol. *72*, 517–549.

Edgar, R.S., Green, E.W., Zhao, Y., van Ooijen, G., Olmedo, M., Qin, X., Xu, Y., Pan, M., Valekunja, U.K., Feeney, K.A., et al. (2012). Peroxiredoxins are conserved markers of circadian rhythms. Nature *485*, 459–464.

Elinav, E., Strowig, T., Kau, A.L., Henao-Mejia, J., Thaiss, C.A., Booth, C.J., Peaper, D.R., Bertin, J., Eisenbarth, S.C., Gordon, J.I., and Flavell, R.A. (2011). NLRP6 inflammasome regulates colonic microbial ecology and risk for colitis. Cell *145*, 745–757.

Fagarasan, S., Muramatsu, M., Suzuki, K., Nagaoka, H., Hiai, H., and Honjo, T. (2002). Critical roles of activation-induced cytidine deaminase in the homeostasis of gut flora. Science *298*, 1424–1427.

Faith, J.J., Guruge, J.L., Charbonneau, M., Subramanian, S., Seedorf, H., Goodman, A.L., Clemente, J.C., Knight, R., Heath, A.C., Leibel, R.L., et al. (2013). The long-term stability of the human gut microbiota. Science *341*, 1237439.

Fonken, L.K., Workman, J.L., Walton, J.C., Weil, Z.M., Morris, J.S., Haim, A., and Nelson, R.J. (2010). Light at night increases body mass by shifting the time of food intake. Proc. Natl. Acad. Sci. USA *107*, 18664–18669.

Gerhart-Hines, Z., Feng, D., Emmett, M.J., Everett, L.J., Loro, E., Briggs, E.R., Bugge, A., Hou, C., Ferrara, C., Seale, P., et al. (2013). The nuclear receptor Rev-erbα controls circadian thermogenic plasticity. Nature *503*, 410–413.

Gordon, J.I. (2012). Honor thy gut symbionts redux. Science *336*, 1251–1253.

Henao-Mejia, J., Elinav, E., Jin, C., Hao, L., Mehal, W.Z., Strowig, T., Thaiss, C.A., Kau, A.L., Eisenbarth, S.C., Jurczak, M.J., et al. (2012). Inflammasome-mediated dysbiosis regulates progression of NAFLD and obesity. Nature *482*, 179–185.

Hogenesch, J.B., and Ueda, H.R. (2011). Understanding systems-level properties: timely stories from the study of clocks. Nat. Rev. Genet. *12*, 407–416.

Hoogerwerf, W.A., Hellmich, H.L., Cornélissen, G., Halberg, F., Shahinian, V.B., Bostwick, J., Savidge, T.C., and Cassone, V.M. (2007). Clock gene expression in the murine gastrointestinal tract: endogenous rhythmicity and effects of a feeding regimen. Gastroenterology *133*, 1250–1260.

Hooper, L.V., Littman, D.R., and Macpherson, A.J. (2012). Interactions between the microbiota and the immune system. Science *336*, 1268–1273.

Hsiao, E.Y., McBride, S.W., Hsien, S., Sharon, G., Hyde, E.R., McCue, T., Codelli, J.A., Chow, J., Reisman, S.E., Petrosino, J.F., et al. (2013). Microbiota modulate behavioral and physiological abnormalities associated with neurodevelopmental disorders. Cell *155*, 1451–1463.

Huang, W., Ramsey, K.M., Marcheva, B., and Bass, J. (2011). Circadian rhythms, sleep, and metabolism. J. Clin. Invest. *121*, 2133–2141.

Hughes, M.E., Hogenesch, J.B., and Kornacker, K. (2010). JTK_CYCLE: an efficient nonparametric algorithm for detecting rhythmic components in genome-scale data sets. J. Biol. Rhythms *25*, 372–380.

Human Microbiome Project Consortium (2012). Structure, function and diversity of the healthy human microbiome. Nature *486*, 207–214.

Johnson, C.H., Egli, M., and Stewart, P.L. (2008). Structural insights into a circadian oscillator. Science *322*, 697–701.

Johnson, C.H., Stewart, P.L., and Egli, M. (2011). The cyanobacterial circadian system: from biophysics to bioevolution. Annu. Rev. Biophys. *40*, 143–167.

Kaasik, K., Kivimäe, S., Allen, J.J., Chalkley, R.J., Huang, Y., Baer, K., Kissel, H., Burlingame, A.L., Shokat, K.M., Ptáček, L.J., and Fu, Y.H. (2013). Glucose sensor O-GlcNAcylation coordinates with phosphorylation to regulate circadian clock. Cell Metab. *17*, 291–302.

Kanehisa, M., and Goto, S. (2000). KEGG: kyoto encyclopedia of genes and genomes. Nucleic Acids Res. *28*, 27–30.

Kanehisa, M., Goto, S., Sato, Y., Kawashima, M., Furumichi, M., and Tanabe, M. (2014). Data, information, knowledge and principle: back to metabolism in KEGG. Nucleic Acids Res. *42* (Database issue), D199–D205.

Keller, M., Mazuch, J., Abraham, U., Eom, G.D., Herzog, E.D., Volk, H.D., Kramer, A., and Maier, B. (2009). A circadian clock in macrophages controls inflammatory immune responses. Proc. Natl. Acad. Sci. USA *106*, 21407–21412.

Lenz, P., and Søgaard-Andersen, L. (2011). Temporal and spatial oscillations in bacteria. Nat. Rev. Microbiol. *9*, 565–577.

Ley, R.E., Turnbaugh, P.J., Klein, S., and Gordon, J.I. (2006). Microbial ecology: human gut microbes associated with obesity. Nature *444*, 1022–1023.

Lozupone, C.A., Stombaugh, J.I., Gordon, J.I., Jansson, J.K., and Knight, R. (2012). Diversity, stability and resilience of the human gut microbiota. Nature *489*, 220–230.

Mohawk, J.A., Green, C.B., and Takahashi, J.S. (2012). Central and peripheral circadian clocks in mammals. Annu. Rev. Neurosci. *35*, 445–462.

Mukherji, A., Kobiita, A., Ye, T., and Chambon, P. (2013). Homeostasis in intestinal epithelium is orchestrated by the circadian clock and microbiota cues transduced by TLRs. Cell *153*, 812–827.

Nguyen, K.D., Fentress, S.J., Qiu, Y., Yun, K., Cox, J.S., and Chawla, A. (2013). Circadian gene Bmal1 regulates diurnal oscillations of Ly6C(hi) inflammatory monocytes. Science *341*, 1483–1488.

Qin, J., Li, R., Raes, J., Arumugam, M., Burgdorf, K.S., Manichanh, C., Nielsen, T., Pons, N., Levenez, F., Yamada, T., et al.; MetaHIT Consortium (2010). A human gut microbial gene catalogue established by metagenomic sequencing. Nature *464*, 59–65.

Rakoff-Nahoum, S., Paglino, J., Eslami-Varzaneh, F., Edberg, S., and Medzhitov, R. (2004). Recognition of commensal microflora by toll-like receptors is required for intestinal homeostasis. Cell *118*, 229–241.

Ridaura, V.K., Faith, J.J., Rey, F.E., Cheng, J., Duncan, A.E., Kau, A.L., Griffin, N.W., Lombard, V., Henrissat, B., Bain, J.R., et al. (2013). Gut microbiota from twins discordant for obesity modulate metabolism in mice. Science *341*, 1241214.

Rust, M.J., Markson, J.S., Lane, W.S., Fisher, D.S., and O'Shea, E.K. (2007). Ordered phosphorylation governs oscillation of a three-protein circadian clock. Science *318*, 809–812.

Scheer, F.A., Hilton, M.F., Mantzoros, C.S., and Shea, S.A. (2009). Adverse metabolic and cardiovascular consequences of circadian misalignment. Proc. Natl. Acad. Sci. USA *106*, 4453–4458.

Silver, A.C., Arjona, A., Walker, W.E., and Fikrig, E. (2012). The circadian clock controls toll-like receptor 9-mediated innate and adaptive immunity. Immunity *36*, 251–261.

So, A.Y., Bernal, T.U., Pillsbury, M.L., Yamamoto, K.R., and Feldman, B.J. (2009). Glucocorticoid regulation of the circadian clock modulates glucose homeostasis. Proc. Natl. Acad. Sci. USA *106*, 17582–17587.

Sommer, F., and Bäckhed, F. (2013). The gut microbiota—masters of host development and physiology. Nat. Rev. Microbiol. *11*, 227–238.

Stecher, B., and Hardt, W.D. (2011). Mechanisms controlling pathogen colonization of the gut. Curr. Opin. Microbiol. *14*, 82–91.

Stokkan, K.A., Yamazaki, S., Tei, H., Sakaki, Y., and Menaker, M. (2001). Entrainment of the circadian clock in the liver by feeding. Science *291*, 490–493.

Suwazono, Y., Dochi, M., Sakata, K., Okubo, Y., Oishi, M., Tanaka, K., Kobayashi, E., Kido, T., and Nogawa, K. (2008). A longitudinal study on the effect of shift work on weight gain in male Japanese workers. Obesity (Silver Spring) *16*, 1887–1893.

Turek, F.W., Joshu, C., Kohsaka, A., Lin, E., Ivanova, G., McDearmon, E., Laposky, A., Losee-Olson, S., Easton, A., Jensen, D.R., et al. (2005). Obesity and metabolic syndrome in circadian Clock mutant mice. Science *308*, 1043–1045.

Yamaguchi, Y., Suzuki, T., Mizoro, Y., Kori, H., Okada, K., Chen, Y., Fustin, J.M., Yamazaki, F., Mizuguchi, N., Zhang, J., et al. (2013). Mice genetically deficient in vasopressin V1a and V1b receptors are resistant to jet lag. Science *342*, 85–90.

Yu, X., Rollins, D., Ruhn, K.A., Stubblefield, J.J., Green, C.B., Kashiwada, M., Rothman, P.B., Takahashi, J.S., and Hooper, L.V. (2013). TH17 cell differentiation is regulated by the circadian clock. Science *342*, 727–730.

EXTENDED EXPERIMENTAL PROCEDURES

Mice

C57Bl/6 mice were purchased from Harlan and allowed to acclimatize to the local animal facility for 2 weeks before used for experimentation. *Per1/2*$^{-/-}$ mice (Adamovich et al., 2014) and *ASC*$^{-/-}$ mice (Sutterwala et al., 2006) have been previously described. Unless otherwise specified, mice were kept under strict light-dark cycles, with lights being turned on at 6am and turned off at 6pm. In all experiments, age- and gender-matched were used. Mice were 8-9 weeks of age at the beginning of experiments. For experiments involving high-fat diet, only male mice were used. For all other experiments, both male and female mice were used. Stool samples were collected fresh and on the basis of individual mice. Fresh pellets were collected in tubes, immediately frozen in liquid nitrogen upon collection, and stored at −80°C until DNA isolation. Unless stated otherwise, 10 mice per experimental group were used for the collection of fecal material from each individual mouse. For the induction of jet lag, mice were shifted between control light conditions (lights turned on at 6am and turned off at 6pm) and an 8 hr time difference (lights turned on at 10pm and turned off at 10am) every 3 days. Experiments performed on jet lagged mice were done when these mice were in the same light-dark cycle as control mice, and ZTs were synchronized (i.e., ZT0 of jet lag mice corresponded to ZT0 of control mice, as all mice were exposed to the same light-dark conditions at the onset of sample collection). In food restriction experiments, mice were housed under standard light-dark conditions (6am to 6pm), but had access to food only during the light or dark phase, respectively, for 2 weeks. For antibiotic treatment, mice were given a combination of vancomycin (1 g/l), ampicillin (1 g/l), kanamycin (1 g/l), and metronidazole (1 g/l) in their drinking water (Rakoff-Nahoum et al., 2004). All antibiotics were obtained from Sigma Aldrich. Antibiotics were given for the entire duration of experiments, i.e., starting at the onset of jet lag induction until the experimental endpoint. Microbial cycling was tested after 1 week of high fat diet or antibiotics treatment, respectively. For experiments involving gnotobiotic mice, germ-free Swiss Webster mice were housed in sterile isolators. For fecal transplantation experiments, 100 mg of stool was resuspended in 1 ml of PBS, homogenized, and filtered through a 70μm strainer. Recipient mice were gavaged with 200μl of the filtrate. All experimental procedures were approved by the local IACUC.

Human Samples

Stool collection from humans was performed using sterile cotton swabs and stored at room temperature until arrival at the laboratory, where DNA extraction was performed. Collection of human stool was approved by the Tel Aviv Sourasky Medical Center Institutional Review Board.

Taxonomic Microbiota Analysis

Frozen fecal samples were processed for DNA isolation using the MoBio PowerSoil kit according to the manufacturer's instructions. 1ng of the purified fecal DNA was used for PCR amplification and sequencing of the bacterial 16S rRNA gene. Amplicons spanning the variable region 1/2 (V1/2) of the 16S rRNA gene were generated by using the following barcoded primers: Fwd 5′-XXXXXXXXA GAGTTTGATCCTGGCTCAG-3′, Rev 5′-TGCTGCCTCCCGTAGGAGT-3′, where X represents a barcode base. The reactions were subsequently pooled in an equimolar ratio, purified (PCR clean kit, Promega), and used for Illumina MiSeq sequencing. 500 bp paired-end sequencing was employed. An in-house script was used to assembly the paired-end reads. Assembly rates of 90% were achieved in all experiments. Reads were then processed using the QIIME (Quantitative Insights Into Microbial Ecology, http://www.qiime.org) analysis pipeline as described (Caporaso et al., 2010; Elinav et al., 2011). In brief, fasta quality files and a mapping file indicating the barcode sequence corresponding to each sample were used as inputs, reads were split by samples according to the barcode, taxonomical classification was performed using the RDP-classifier, and an OTU table was created. We employed closed-reference OTU mapping using the Greengenes database. The number of allowed non-matching nucleotides was between 0 and 5 on a total paired-end assembled read length of 359bp. After chimera removal, the average number of reads per fecal sample was 34,847. Rarefaction was performed to exclude samples with insufficient reads per sample counts. Sequences sharing 97% nucleotide sequence identity in the V2 region were binned into operational taxonomic units (97% ID OTUs). Chao1 index was calculated to depict alpha-diversity. For beta-diversity, unweighted unifrac measurements were plotted according to the first two principal coordinates based on 1,000 reads per sample. The OTU tables used for our analyses are made accessible online.

Metagenomic Sequence Mapping

Illumina sequencing reads were mapped to a gut microbial gene catalog (Qin et al., 2010) using GEM mapper (Marco-Sola et al., 2012) with the following parameters:

-m 0.08 – s 0 – q offset-33 – gem-quality-threshold 26

Functional Assignment

Reads mapped to the gut microbial gene catalog were assigned a KEGG (Kanehisa and Goto, 2000; Kanehisa et al., 2014) identification number, according to the gene to category mapping that accompanied the gene catalog. Genes were subsequently mapped to KEGG modules and pathways. For the KEGG pathway analysis, only pathways whose gene coverage was above 0.2 were included. KEGG pathways were then tested by JTK_cycle for daily oscillations.

Statistical Analysis

Data are expressed as mean ± SEM. For the analysis of rhythmic oscillations and their amplitudes, the non-parametric test JTK_cycle was used (Hughes et al., 2010), incorporating a window of 18-24 hr for the determination of circadian periodicity. Bonferroni-adjusted P values < 0.05 were considered significant. The Benjamini-Hochberg procedure was used to control the false discovery rate. JTK_cycle results are provided in supplemental tables. Differences in metabolic data were analyzed by ANOVA, and post-hoc analysis for multiple group comparison was performed. Pairwise comparison between host transcript data was performed using Student's t test. ANOVA and t test were performed using GraphPad Prism software.

Glucose Tolerance Test

Mice were fasted for 6 hr and subsequently given 200μl of a 0.2g/ml glucose solution (JT Baker) by oral gavage. Blood glucose was determined at 0, 15, 30, 60, 90, and 120 min after glucose challenge (Contour blood glucose meter, Bayer, Switzerland).

MRI

Mice were anesthetized with isofluorane (5% for induction, 1%–2% for maintenance) mixed with oxygen (1 l/min) and delivered through a nasal mask. Once anesthetized, the animals were placed in a head-holder to assure reproducible positioning inside the magnet. Respiration rate was monitored and kept throughout the experimental period around 60–80 breaths per minute. MRI experiments were performed on 9.4 Tesla BioSpec Magnet 94/20 USR system (Bruker, Germany) equipped with gradient coils system capable of producing pulse gradient of up to 40 gauss/cm in each of the three directions. All MR images had been acquired with a quadrature resonator coil (Bruker). The MRI protocol included two sets of coronal and axial multi-slices T2-weighted MR images. The T2-weighted images acquired using the multi-slice RARE sequence (TR = 2500 ms, TE = 35 ms, RARE factor = 8), and matrix size was 256 × 256, four averages, corresponding to an image acquisition time of 2 min 40 s per set. The first set was used to acquire 21 axial slices with 1.00 mm slice thickness (no gap). The field of view was selected with 4.2 × 4.2 cm^2. The second set was used to acquire 17 coronal slices with 1.00 mm slice thickness (no gap). The field of view was selected with 7.0 × 5.0 cm^2.

Total fat and lean mass of mice were measured by EchoMRI-100™ (Echo Medical Systems, Houston, TX).

Metabolic Studies

Food intake and locomotor activity were measured using the PhenoMaster system (TSE-Systems, Bad Homburg, Germany), which consists of a combination of sensitive feeding sensors for automated measurement and a photobeam-based activity monitoring system detects and records ambulatory movements, including rearing and climbing, in each cage. All parameters were measured continuously and simultaneously. Mice were trained singly-housed in identical cages prior to data acquisition.

Gene Expression Analysis

Tissues were preserved in RNAlater solution (Ambion) and subsequently homogenized in Trizol reagent (Invitrogen). Cells sorted by FACS were resuspended in Trizol reagent. RNA was purified according to the manufacturer's instructions. One microgram of total RNA was used to generate cDNA (HighCapacity cDNA Reverse Transcription kit; Applied Biosystems). RealTime-PCR was performed using gene-specific primer/probe sets (Applied Biosystems) and Kapa Probe Fast qPCR kit (Kapa Biosystems) on a Viia7 instrument (Applied Biosystems). PCR conditions were 95°C for 20 s, followed by 40 cycles of 95°C for 3 s and 60°C for 30 s. Data were analyzed using the deltaCt method with hprt1 serving as the reference housekeeping gene.

SUPPLEMENTAL REFERENCES

Caporaso, J.G., Kuczynski, J., Stombaugh, J., Bittinger, K., Bushman, F.D., Costello, E.K., Fierer, N., Peña, A.G., Goodrich, J.K., Gordon, J.I., et al. (2010). QIIME allows analysis of high-throughput community sequencing data. Nat. Methods *7*, 335–336.

Marco-Sola, S., Sammeth, M., Guigó, R., and Ribeca, P. (2012). The GEM mapper: fast, accurate and versatile alignment by filtration. Nat. Methods *9*, 1185–1188.

Sutterwala, F.S., Ogura, Y., Szczepanik, M., Lara-Tejero, M., Lichtenberger, G.S., Grant, E.P., Bertin, J., Coyle, A.J., Galán, J.E., Askenase, P.W., and Flavell, R.A. (2006). Critical role for NALP3/CIAS1/Cryopyrin in innate and adaptive immunity through its regulation of caspase-1. Immunity *24*, 317–327.

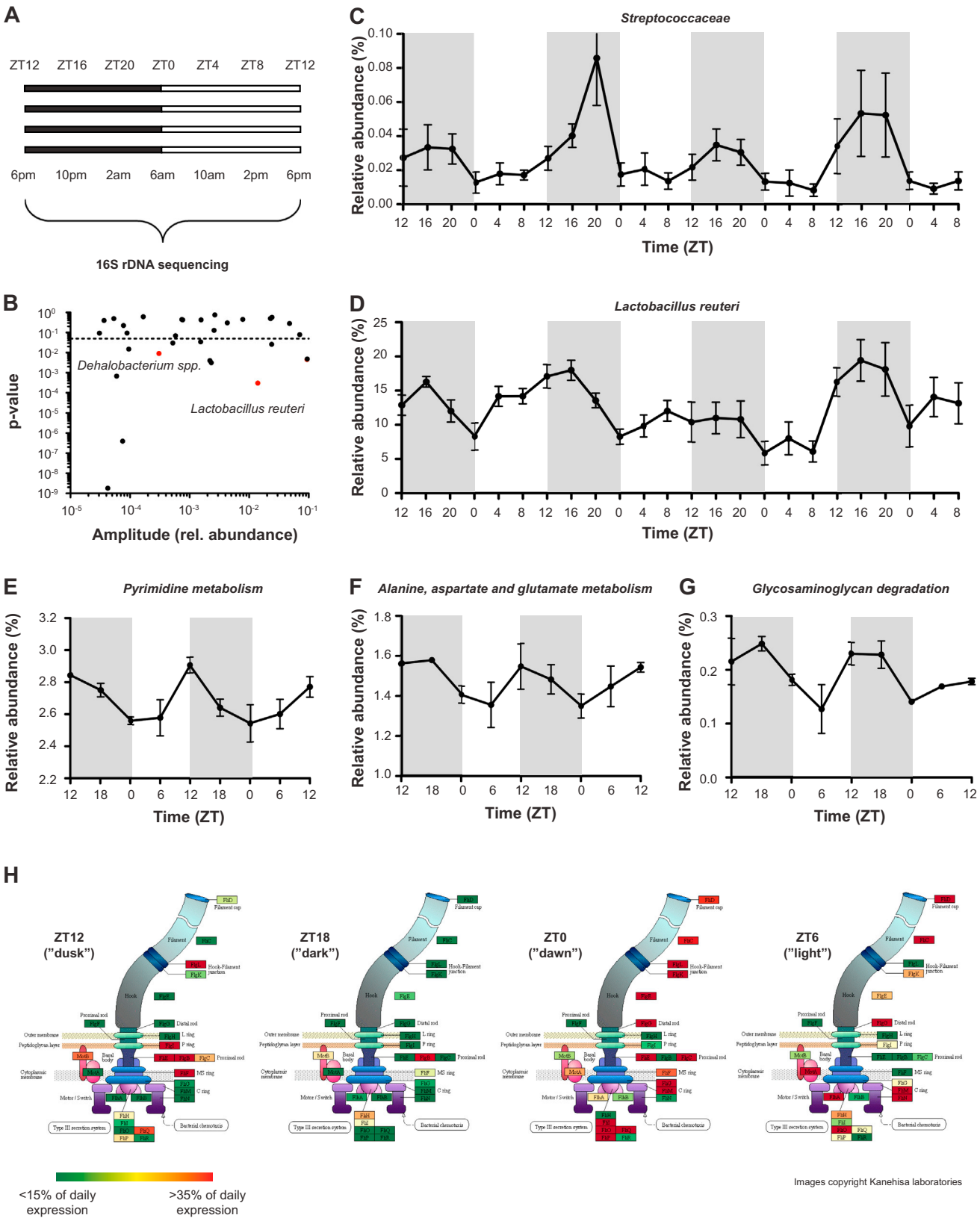

(legend on next page)

Figure S1. Diurnal Microbiota Oscillations in Composition and Function, Related to Figure 1

(A) Schematic showing sampling times of microbiota every four hours over the course of four light-dark cycles.

(B) OTUs showing diurnal oscillations. Dashed line indicates $p < 0.05$, JTK_cycle; n = 8 individual mice at each time point.

(C and D) Representative examples of diurnal oscillations in the abundance of microbiota members; n = 8 mice at each time point.

(E–G) Representative examples of diurnal oscillations in the abundance of functional KEGG pathways; n = 2 individual mice at each time point.

(H) Pathway depiction of genes involved in flagellar assembly, type III secretion system, and bacterial chemotaxis. Colors indicate differential abundance of genes at different Zeitgeber times (ZTs).

Data are expressed as mean ± SEM.

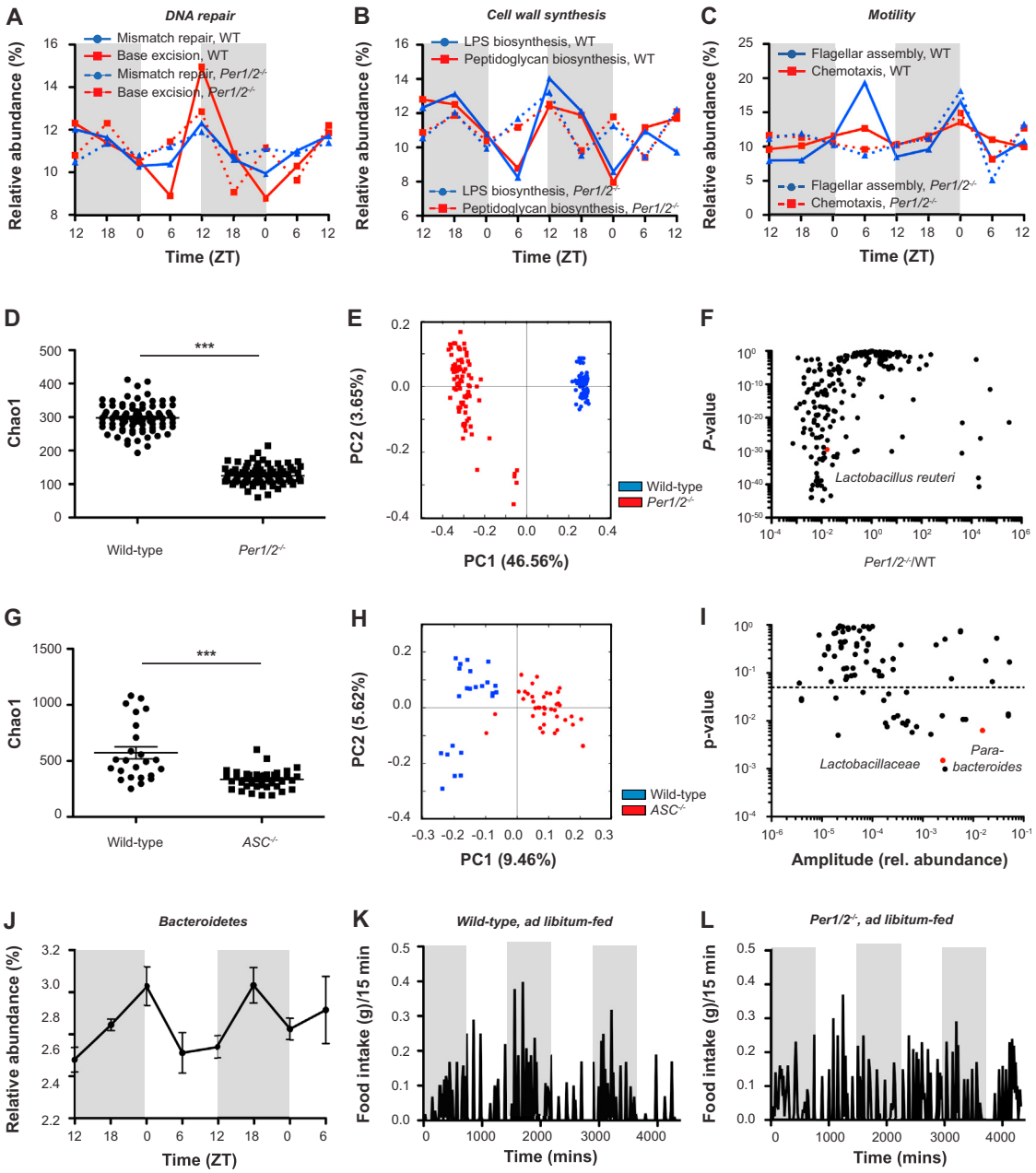

Figure S2. Dysbiosis in *Per1/2*-Deficient Mice, Related to Figure 2

(A–C) Diurnal variations in genes belonging to the indicated functional pathways in wild-type and *Per1/2*-deficient mice. Metagenomic analysis was performed in a total of three mice at each time point.

(D and E) Alpha- (D) and beta-diversity (E) of fecal microbiota from wild-type and *Per1/2*-deficient mice. Samples per genotype are from different times of the day; n = 90 in each group. ***$p < 0.001$

(F) Differential abundance of OTUs between fecal microbiota from wild-type and *Per1/2*-deficient mice; n = 90 samples.

(G and H) Alpha- (G) and beta-diversity (H) of fecal microbiota from wild-type and *ASC*-deficient mice. ***$p < 0.001$

(I) OTUs showing diurnal oscillations in *ASC*-deficient mice. Dashed line indicates $p < 0.05$, JTK_cycle; n = 8 individual mice at each time point.

(J) Representative example of diurnal oscillations in the microbiota of *ASC*-deficient mice; n = 8 individual mice at each time point.

(K and L) Diurnal feeding pattern in wild-type (K) compared to *Per1/2*-deficient mice (L). Mice were fed ad libitum and followed over three dark-light cycles. Examples shown are representative of 8 individual mice.

Data are expressed as mean ± SEM.

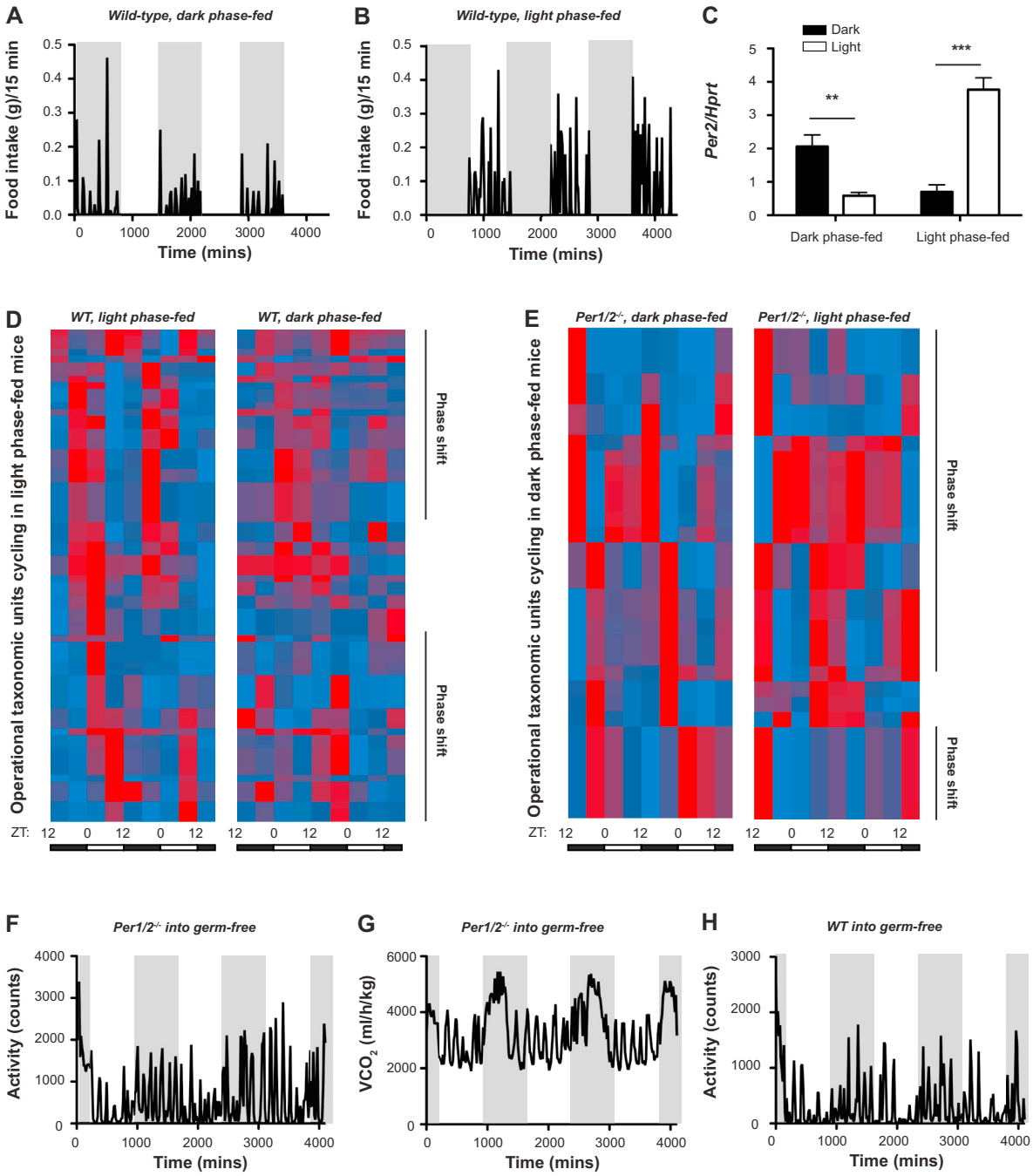

Figure S3. The Impact of Feeding Rhythms on Diurnal Microbiota Oscillations, Related to Figure 3

(A and B) Feeding times in dark-phase-fed (A), and light-phase-fed (B) mice. Graphs shown are representative of four individual mice measured.

(C) Colonic expression of *Per2* in dark-phase-fed or light-phase-fed mice during the dark phase and light phase shows reprograming of the intestinal clock by feeding rhythms; n = 10 mice in each group; $^{**}p < 0.01$, $^{***}p < 0.001$

(D and E) Heatmap representation of bacterial genera oscillating with $p < 0.05$, JTK_cycle, in wild-type mice (D) and *Per1/2*-deficient mice (E) fed during the dark phase or light phase only; n = 10 mice at each time point. Phase shifts in cycling OTUs are highlighted.

(F–H) Physical activity (F, H) and VCO_2 (G) over the course of three dark-light cycles in germ-free mice transplanted with microbiota from *Per1/2*-deficient mice (F, G) or from wild-type mice (H). Measurements were taken 1 week after fecal transplantation. The graph is representative of eight individual mice measured.

Data are expressed as mean ± SEM.

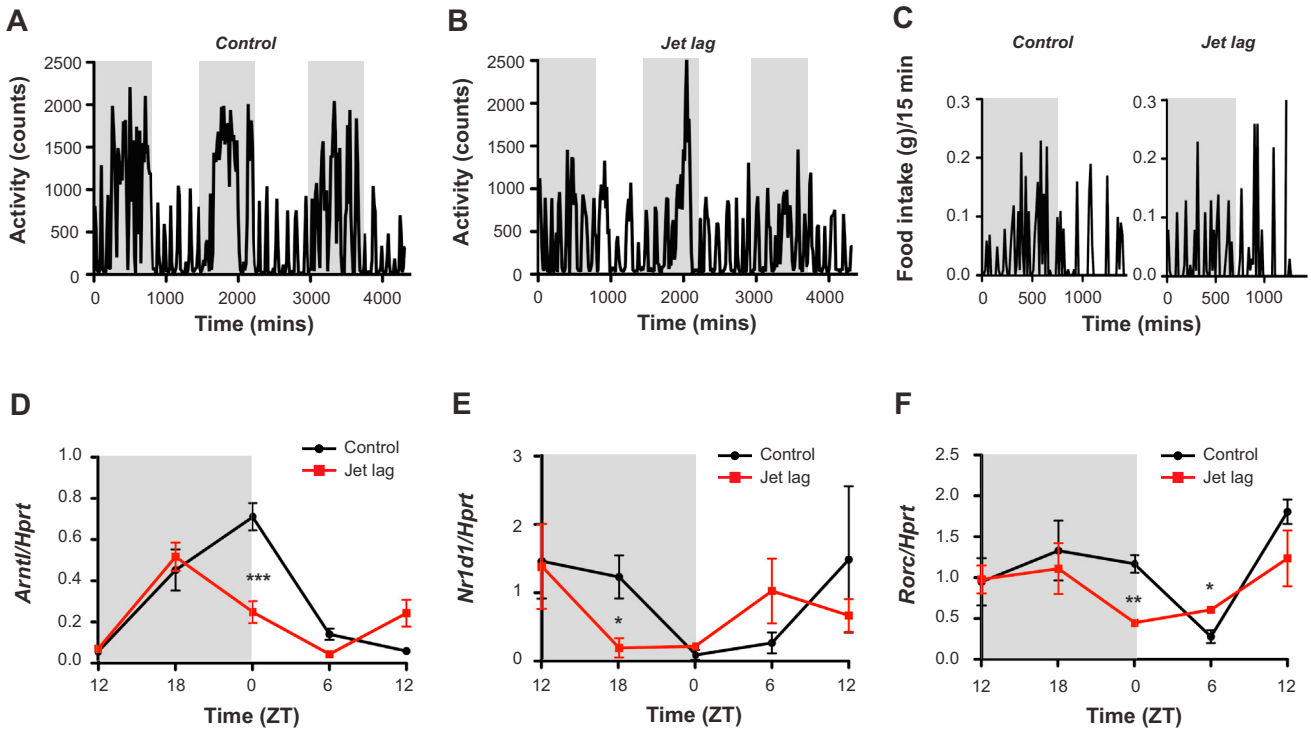

Figure S4. Circadian Misalignment during Jet Lag, Related to Figure 4

(A and B) Physical activity over the course of three dark-light cycles in control and jet lag mice. Rhythmic activity of a control mouse (A) is converted into a random pattern by induction of jet lag (B). The results shown are representative of 16 individual mice measured.

(C) Diurnal variations in food intake of control and jet lag mice over the course of a dark-light cycle. The results shown are representative of 16 individual mice measured.

(D–F) Rhythmic expression patterns of Bmal (D), Rev-erbα (E) and RORγt (F) in the colon is altered upon jet lag induction; n = 4-5 mice at each time point. Data are expressed as mean ± SEM.

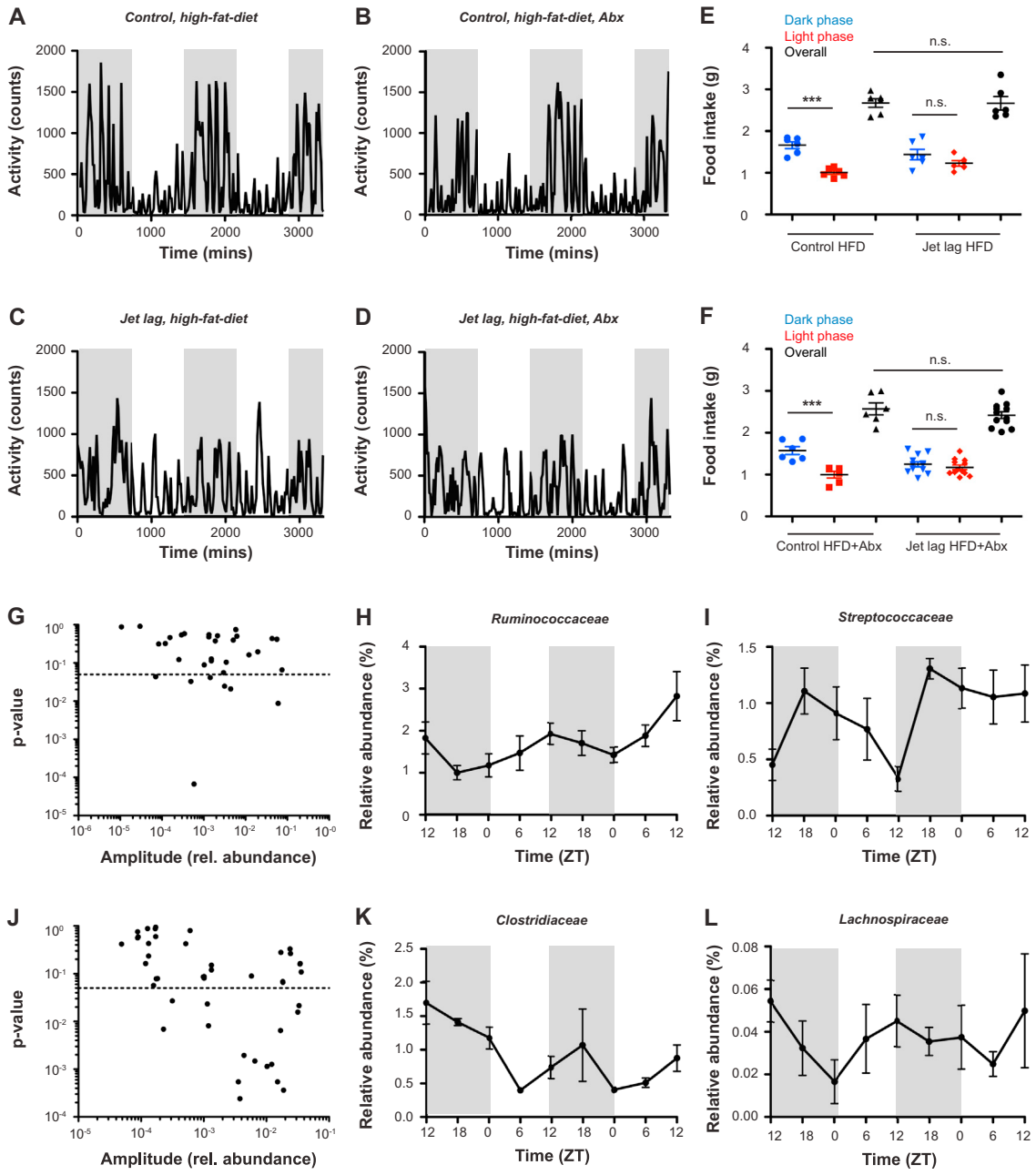

Figure S5. The Effect of High-Fat Diet and Antibiotic Treatment on Diurnal Behavior and Microbiota Oscillations, Related to Figure 5

(A–D) Physical activity over the course of 2.5 dark-light cycles in control (A, B) and jet lag mice (C, D) fed a high-fat diet. (B) and (D) are additionally treated with antibiotics. The results shown are representative of 32 individual mice measured.

(E and F) Diurnal variations in food intake of control and jet lag mice over the course of a dark-light cycle. All mice were fed a high-fat diet. In (F), mice were treated with antibiotics.

(G) OTUs showing diurnal oscillations in wild-type mice after 1 week on high-fat diet. Dashed line indicates $p < 0.05$, JTK_cycle; n = 10 individual mice at each time point.

(H and I) Representative examples of diurnal oscillations in the abundance of microbiota members in mice on high-fat diet; n = 10 mice at each time point.

(J) OTUs showing diurnal oscillations in wild-type mice after 1 week of antibiotic treatment. Dashed line indicates $p < 0.05$, JTK_cycle; n = 10 individual mice at each time point.

(K and L) Representative example of diurnal oscillations in the abundance of microbiota members in mice on antibiotics; n = 10 mice at each time point.

Data are expressed as mean ± SEM.

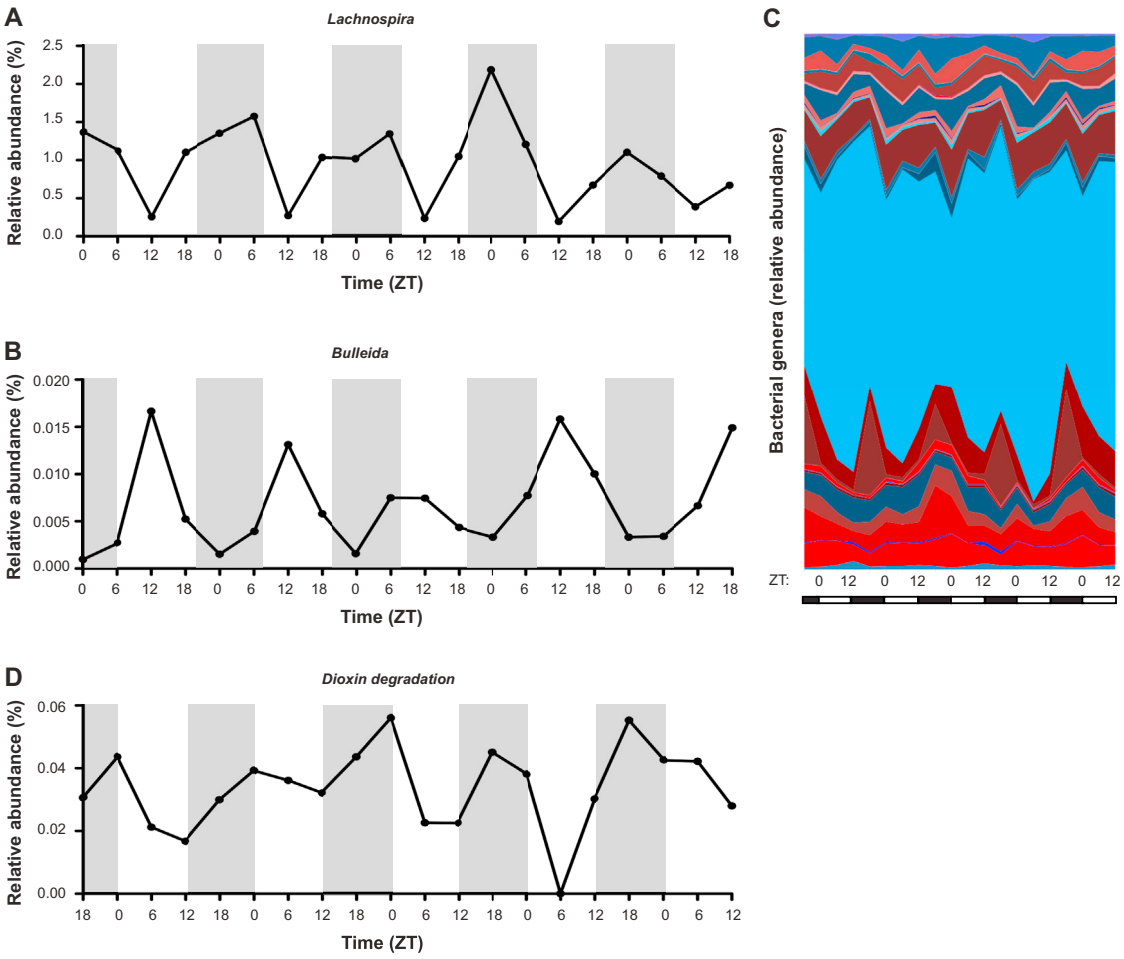

Figure S6. Diurnal Oscillations in the Composition and Function of Human Microbiota, Related to Figure 6

(A and B) Representative examples of diurnal fluctuations in the relative abundance of members of the commensal microbiota from one human subject over the course of 5 consecutive days.

(C) Oscillations in taxonomic composition of human fecal microbiota over the course of 5 days.

(D) Representative examples of diurnal fluctuations in functional pathways from human microbiota over the course of 5 consecutive days.

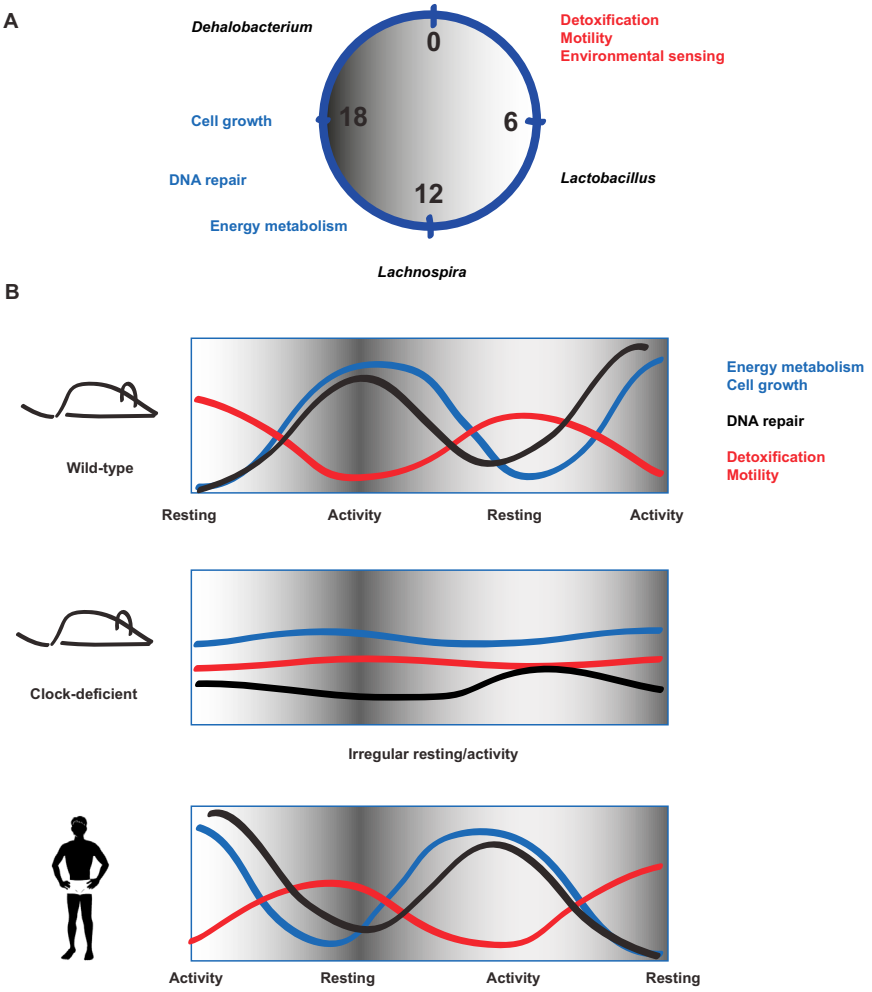

Figure S7. Schematic of Diurnal Oscillations in Microbiota Composition and Function, Related to Figure 7

(A) Schematic showing "hallmark" taxonomic units and functional pathways with preferential abundance at certain times during a 24 hr light-dark cycle.

(B) Schematic depicting diurnal microbiota pathway activity in nocturnal wild-type mice, loss of oscillations in clock-disrupted mice, and phase-reversed fluctuations in humans.